

Linköping Studies in Science and Technology
Dissertation No. 1056

Studies of Charge Transport and Energy Level in Solar Cells Based on Polymer/Fullerene Bulk Heterojunction

Abay Gadisa



Linköping University
INSTITUTE OF TECHNOLOGY

Biomolecular and Organic Electronics
Department of Physics, Chemistry and Biology
Linköping University, SE-581 83 Linköping, Sweden

Linköping 2006

ISBN: 91-85643-51-3
ISSN 0345-7524
Printed by LiU-Tryck, Linköping, Sweden 2006

Abstract

π -Conjugated polymers have attracted considerable attention since they are potential candidates for various opto-electronic devices such as solar cells, light emitting diodes, photodiodes, and transistors. Electronic devices based on conjugated polymers can be easily processed at low temperature using inexpensive technologies. This leads to cost reduction, a key-deriving factor for choosing conjugated polymers for various types of applications. In particular, polymer based solar cells are of special interest due to the fact that they can play a major role in generating clean and cheap energy in the future.

The investigations described in thesis are aimed mainly at understanding charge transport and the role of energy levels in solar cells based on polymer/acceptor bulk heterojunction (BHJ) active films. Best polymer based solar cells, with efficiency 4 to 5%, rely on polymer/fullerene BHJ active films. These solar cells are in an immature state to be used for energy conversion purposes. In order to enhance their performance, it is quite important to understand the efficiency-limiting factors. Solid films of conjugated polymers compose conjugation segments that are randomly distributed in space and energy. Such distribution gives rise to the localization of charge carriers and hence broadening of electron density of states. Consequently, electronic wave functions have quite poor overlap resulting into absence of continuous band transport. Charge transport in polymers and organic materials, in general, takes place by hopping among the localized states. This makes a bottleneck to the performance of polymer-based solar cells. In this context, the knowledge of charge transport in the solar cell materials is quite important to develop materials and device architectures that boost the efficiency of such solar cells.

Most of the transport studies are based on polyfluorene copolymers and fullerene electron acceptor molecules. Fullerenes are blended with polymers to enhance the dissociation of excited state into free carriers and transport free electrons to the respective electrode. The interaction within the polymer-fullerene complex, therefore, plays a major role in the generation and transport of both electrons and holes. In this thesis, we present and discuss the effect of various polymer/fullerene compositions on hole percolation paths. We mainly focus on hole transport since its mobility is quite small as compared to electron mobility in the fullerenes, leading to creation of space charges within the bulk of the solar cell composite. Changing a polymer band gap may necessitate an appropriate acceptor type in order to fulfill the need for sufficient driving force for dissociation of photogenerated electron-hole pairs. We have observed that different acceptor types give rise to completely

different hole mobility in BHJ films. The change of hole transport as a function of acceptor type and concentration is mainly attributed to morphological changes. The effect of the acceptors in connection to hole transport is also discussed. The later is supported by studies of bipolar transport in pure electron acceptor layers. Moreover, the link between charge carrier mobility and photovoltaic parameters has also been studied and presented in this thesis.

The efficiency of polymer/fullerene-based solar cells is also significantly limited by its open-circuit voltage (V_{oc}), a parameter that does not obey the metal-insulator-metal principle due to its complicated characteristics. In this thesis, we address the effect of varying polymer oxidation potential on V_{oc} of the polymer/fullerene BHJ based solar cells. Systematic investigations have been performed on solar cells that comprise several polythiophene polymers blended with a fullerene derivative electron acceptor molecule. The V_{oc} of such solar cells was found to have a strong correlation with the oxidation potential of the polymers. The upper limit to V_{oc} of the aforementioned solar cells is thermodynamically limited by the net internal electric field generated by the difference in energy levels of the two materials in the blend.

The cost of polymer-based solar cells can be reduced to a great extent through realization of all-plastic and flexible solar cells. This demands the replacement of the metallic components (electrodes) by highly conducting polymer films. While hole conductor polymers are available, low work function polymer electron conductors are rare. In this thesis, prototype solar cells that utilizes a highly conducting polymer, which has a work function of ~ 4.3 eV, as a cathode are demonstrated. Development of this material may eventually lead to fabrication of large area, flexible and cheap solar cells. The transparent nature of the polymer cathode may also facilitate fabrication of multi-layer and tandem solar cells.

In the last chapter of this thesis, we demonstrate generation of red and near infrared polarized light by employing thermally converted thin films of polyfluorene copolymers in light emitting diodes. This study, in particular, aims at fabricating polarized infrared light emitting devices.

Preface

The investigations addressed in this thesis have been carried out in the Biomolecular and Organic Electronics group, at the division of Applied Physics, Department of Physics, Chemistry, and Biology, Linköping University, Sweden. The Biomolecular and Organic Electronics group is one of the research groups that have made a profound contribution to the field of polymer electronics. Among the ongoing research activities within this group, the research on polymer based solar cells is a typical example. I was enrolled as a PhD student in September 2002, with the aim of investigating efficiency limiting factors in solar cells based on polymer/acceptor active layer and developing efficient solar cells using the knowledge and experience gained thereof. All the research activities discussed in this thesis have involved the effort, experience and cooperation of several people and laboratories, whereby my supervisor Prof. Olle Inganäs has facilitated all the networks.

Most of the investigations and discussions presented in the thesis are targeting at addressing the charge transport and energy levels and their correlation to photovoltaic parameters. The issue of charge transport in organic materials is quite different from that of crystalline inorganic semiconductors, which have a defined band transport. The amorphous nature of organic films gives rise to hopping transport characterized by considerable activation energies. The charge transport studies composed in this thesis have unveiled several useful information that helps engineering material combinations, synthesis and device architecture. Moreover, since efficient polymer based solar cells rely on donor/acceptor blends, it is important to understand the correlation of the energy levels of these materials with the photovoltaic parameters of the solar cells; issues related to open circuit voltage are discussed in detail.

During the long study period, I haven't restricted myself to one single project but involved in several different activities-thanks to the flexible working environments. As a result, I have been involved in developing solar cells that utilize transparent polymer electrodes, with the aim of constructing an all-plastic solar cell. Part of a work presented in this thesis also involves generation of polarized light making use of thermally converted liquid crystalline polymer films.

Abay Gadisa
Linköping, November 2006

List of articles included in the thesis

Article I

A. Gadisa, M. Svensson, M. R. Andersson, and O. Inganäs, *Correlation between oxidation potential and open-circuit voltage of composite solar cells based on blends of polythiophenes/fullerene derivative*, Appl. Phys. Lett. **84**, 1609-1611 (2004).

Article II

A. Gadisa, X. Wang, S. Admassie, E. Perzon, F. Oswald, F. Langa, Mats R. Andersson, and O. Inganäs, *Stoichiometry dependence of charge transport in polymer/methanofullerene and polymer/C₇₀ derivative based solar cells*, Org. Electron. **7**, 195-204 (2006).

Article III

A. Gadisa, F. Zhang, D. Sharma, M. Svensson, Mats R. Andersson, and O. Inganäs, *Improvements of fill factor in solar cells based on blends of polyfluorene copolymers as electron donors*, Thin Solid Films, In press.

Article IV

A. Gadisa, X. Wang, K. Tvingstedt, F. Oswald, F. Langa, and O. Inganäs, *Bipolar transport and infrared light emission in C₆₀ and C₇₀ derivative electron acceptors*, Appl. Phys. Lett., Submitted.

Article V

A. Gadisa, K. Tvingstedt, S. Admassie, L. Lindell, X. Crispin, Mats R. Andersson, W.R Salaneck, and O. Inganäs, *Transparent polymer cathode for organic photovoltaic devices*, Synth. Met. **156**, 1102-1107 (2006).

Article VI

A. Gadisa, E. Perzon, mats R. Andersson, and O. Inganäs, *Red and near infrared polarized light emission from polyfluorene copolymer based light emitting diodes*, Manuscript.

My contributions to the articles included in the thesis

Article I

All of the experimental work and the writing

Article II

All of the experimental work and the writing

Article III

All of the experimental work and the writing

Article IV

Most of the experimental work and the writing

Article V

Most of the experimental work and the writing

Article VI

All of the experimental work and the writing

Articles to which I have contributed but not included in the thesis

Article VII

F. Zhang, A. Gadisa, O. Inganäs, M. Svensson, and M. R. Andersson, *Influence of buffer layers on the performance of polymer solar cells*, Appl. Phys. Lett. **84**, 3906-3908 (2004).

Article VIII

O. Inganäs, M. Svensson, F. Zhang, A. Gadisa, N.K. Persson, X. Wang, and M.R. Andersson, *Low bandgap alternating polyfluorene copolymers in plastic photodiodes and solar cells*, Appl. Phys. A-Mater.Sci. Process. **79**, 31-35 (2004).

Article IX

K.G. Jespersen, F. Zhang, A. Gadisa, V. Sundström, A. Yartsev, and O. Inganäs, *Charge formation and transport in bulk-heterojunction solar cells based on alternating polyfluorene copolymers blended with fullerenes*, Org. Electron. **7**, 235-242 (2006).

Contribution to a book chapter

O. Inganäs, F. Zhang, X. Wang, A. Gadisa, N.K. Persson, M. svensson, E. Perzon, W. Mammo, and M.R. Andersson, *Alternating polyfluorene copolymer-fullerene blend solar cells*, Organic photovoltaics: mechanisms, materials, and devices, ed S.-Shajing Sun and N.S. Sariciftci, Taylor & Francis Inc. (2005).

Acknowledgements

Pursuing a PhD in a group engaged in multidisciplinary research activities gave me an opportunity to work with several people of various background and experience. In particular, the discussions, collaborative research activities, and meetings have left me with tremendous experiences. I have now come to the end of my journey and finally take this opportunity to express my gratitude to friends, colleagues, collaborators, etc who have contributed to the completion of this thesis.

I am principally quite grateful to my supervisor Prof. Olle Inganäs for the excellent guidance, encouragement and helps of all sorts. I have learnt a lot from all the discussions we have made in your office, in the research labs, on the lakes and countryside.

I am quite indebted to the International programme in Physical Sciences (IPPS) of Uppsala University, Sweden for the full financial support. I would like to thank all the IPPS's staffs for their continuous care and support throughout my study period.

All the present and former members of Biorgel group: you all have made my life enjoyable in one-way or another. Apart from the scientific collaborations and discussions, I have enjoyed all the activities I have participated in; the bowling, badminton and parties of various forms are unforgettable. In particular, I am indebted to my colleagues in Organic Electronic group for the wonderful collaborations.

I am quite lucky having nice friends who made my life easier and enjoyable. Fredrik Karlsson, you are a wonderful friend. You have made my life sweat when I was quite alone during my first winter experience; the New Year party was remarkable. I am quite grateful to Seifu Belew for guiding me in Linköping as well as Stockholm. You and your friends, Belay and Mesfine, made my time in Stockholm enjoyable. I thank all my friends who live elsewhere but supported me in many ways. In particular, the endless support I got from Tesfaye Ayalew is exceptional. You and Marr are quite great friends. Eyob Alebachew, your contributions are countless. Thanks a lot. Solomon Fekade, thank you for all your encouragements.

I am indebted to the synthesis group at Chalmers University of Technology, Prof. Mats R. Andersson, Dr. Matias Svensson, and Erik Perzon for providing us with wonderful polymers of various colours.

I am grateful to all the people in IFM. In particular, to Bo Thunér for all the technical assistance and for arranging all the tours around Linköping in winter as well as

summer; to Ann-Marie Holm and Dr. Stefan Welin Klintström for all the administrative assistances.

I am also quite grateful to Dr. Bantikassegn Workalemahu who initiated my study. The advices and supports of Dr. Mulugeta Bekele, Dr. Wondemagegn Mamo, and Dr. Shimelis Admassie were valuable. Thank you all.

Meseret Gadisa, Aynalem Gadisa, and Teshome Korme: You are quite special people who have helped me a lot in many ways. Thank you a lot.

Last but not list, quite special thanks goes to my wife Mihret Yohannes for the incredible support and care you gave me. Your patience and dedication have been terrific. I have only little space and cannot list all you have done for me but thank you a lot Merry.

/Abay Gadisa

Contents

1. General introduction	1
2. Conjugated polymers: electrical, optical and morphological properties	4
2.1 The origin of semiconducting behavior	4
2.2 Correlation of chain distributions and optical phenomena	8
2.3 Morphology of thin conducting polymer films	9
3. Donor/acceptor bulk heterojunction (BHJ) based solar cells	11
3.1 Working principles	11
3.2 The current-voltage (I-V) characteristics	13
3.3 Efficiency limiting factors	15
4. The origin of open-circuit voltage in BHJ based solar cells	17
5. Charge carrier transport models and mobility measurement techniques	21
5.1 Models of hopping transport	21
5.2 Typical experimental mobility measurement techniques	25
6. The method of space charge limited current	27
6.1 Extraction of transport parameters from I-V characteristics	27
6.1.1 Typical features of I-V characteristics measured in the dark	27
6.1.2 Formulation of space charge limited current model	29
6.2 Carrier transport study using unipolar sandwich structure devices	31
6.2.1 The concept of single carrier devices	31
6.2.2 Hole transport in alternating polyfluorene copolymers (APFO)	32
6.2.3 Hole transport in blends of APFOs and acceptor molecules	36
6.3 Bipolar transport in pristine acceptor molecules and its implication for charge transport in polymer/acceptor BHJ based solar cells	39
7. Transparent polymer cathode: Towards all-polymer solar cells	43
8. Polarized light emission from APFOs	48
References	53

1. General introduction

The vast portion of global energy production comes from fossil fuel, while other forms of energy contributes comparatively smaller percentage. However, due to the predicted end of fossil energies, such as oil and the long-term effect of carbon dioxide, renewable energy sources have been considered as the best alternatives. Among the renewable energy sources, the most abundant, but not yet utilized well is the solar energy. The freely available solar energy can directly be converted into electricity by a photovoltaic device (PVD). Conventional PVDs are fabricated from inorganic semiconductor materials such as crystalline silicon (Si) and they are already available on the market. Fabrication of inorganic semiconductor based solar cells demands expensive technologies for purification, patterning and various coating processes. As a result, the inorganic PVDs are quite expensive and hardly compute with other conversional energy sources.

If photovoltaic devices are to be considered as the major future global energy sources, large-scale manufacturing at reasonably low cost is desired. The cost reduction can be realized by using semiconducting materials that can be processed using few steps and cheap technologies. Thus, there has been considerable effort in developing thin film technologies that enable significant cost reductions. In the last few years, solar cells based on thin and multijunction inorganic films have emerged as alternatives to crystalline Si based solar cells. These solar cells are fabricated by using cheap techniques such as sputtering and physical vapor deposition. Currently, they are relatively cheaper but less efficient as compared to Si based solar cells. In general, achieving competitive, cost effective and efficient PVDs may require new materials, concepts and technologies.

Conducting organic materials, in particular π -conjugated polymers, have emerged as a new class of semiconductors that have vital use in various opto-electronic devices. The first class of conducting polymers were discovered in 1977 when high conductivity was observed in doped polyacetylene.¹ This marked the beginning of the era of the new class of semiconductor materials, which are typically inexpensive and easy to process. Polymeric semiconductors can be processed from solutions by spin coating or printing techniques and hence are one of the best choices for construction of large area and flexible electronic devices. In addition, the functionality of conducting conjugated polymers can easily be tailored through careful molecular design and synthesis giving rise to various types of polymers with specific optical and electrical properties.

The field of conjugated polymer-based electronics is rapidly expanding in areas wherever low cost, flexibility and lightweight is desirable. Currently, conjugated polymers have become candidates for several applications such as PVDs,^{2, 3} integrated electronic circuits based on field effect transistors^{4,5} and flat displays based on light emitting diodes⁶.

To fulfill the future energy needs, flexible and cheap polymer solar cells (PSC) are considered as potentially viable devices. Best performing PSCs rely on a bulk heterojunction (BHJ) network of polymer/molecule blends, which is usually sandwiched between two asymmetric metals acting as anode and cathode. In such films, photo generated electron-hole pairs (excitons) are separated at the donor (polymer)/acceptor (molecule) (D/A) interface and the free carriers are collected by the respective electrodes. BHJ films are processed from solutions mainly through spin coating method, which is quite easy and cheap.^{2,3} The top electrode (cathode) of BHJ based PSC, in most cases, is constructed through thermal evaporation techniques while the bottom electrode (anode) is constructed from a glass or plastic substrate coated with thin conducting films. Despite the facts that the processing conditions of BHJ based PSC are easy and cheap, the physics underlying the working principles of these devices is quite complex.

In this thesis, several issues concerning the photovoltaic parameters of solar cells with polymer/acceptor BHJ films are addressed. One of the main parameters limiting the efficiency of the D/A based PSC is the open-circuit voltage (V_{oc}). Unlike that of traditional inorganic solar cells, the V_{oc} of the aforementioned PVDs does not obey the metal-insulator-metal (MIM) principle, but it is rather a complicated function of interface conditions,⁷ electronic levels⁸ and morphology⁹ of the BHJ composites. Here, we address the strong correlation between the V_{oc} of BHJ solar cells and the highest occupied molecular orbital (HOMO) of the conjugated polymer in the D/A layer. Charge carrier transport is another key parameter that influences the efficiency of BHJ polymer solar cells. A part of this thesis is dedicated to description of charge carrier transport in thin polymer as well as BHJ films in a solar cell configuration. The transport parameters and their relation to inherent material parameters are addressed based on experimental data and theoretical models of charge transport in disordered medias. The effect of charge transport on efficiency of solar cells is quite tremendous. In particular, as far as PSCs are concerned, the low hole mobility in most conjugated polymers contributes a lot towards reduction of power conversion efficiency. Luckily enough, hole transport in most polymer/acceptor BHJ films is enhanced mainly due to morphological changes. As will be discussed in this thesis,

the electron acceptor molecules have bipolar transport behavior, which makes them possible pathways for both electrons and holes.

Conducting polymers can be considered as potentially useful materials to fabricate large area and flexible solar cells. An all-polymer solar cell fulfills the criteria of flexibility and low cost. Such solar cells can be realized by replacing metallic electrodes with transparent, conducting polymer electrodes. In this thesis, a vapor phase polymerized transparent polymer layer is suggested as a cathode for sandwich structure devices. This electron conducting polymer is integrated into solar cells by a soft contact lamination technique.

The charge transport studies mainly covers a family of interesting copolymers known as polyfluorene copolymers (APFO). APFOs are a class of copolymers that possess several phases, including thermotropic liquid crystalline phases. Liquid crystalline materials are quite interesting because of their essential application in display devices. The APFO copolymers possess liquid crystalline phases as observed under thermal treatments. Thermally converted thin films of APFOs show anisotropy in optical absorption and photoluminescence. Light emitting diodes based on such films emit polarized light. In the last chapter of this thesis, we demonstrate light-emitting diodes that emit polarized light in the red and near infrared regions.

2. Conjugated polymers: electrical, optical and morphological properties

- ❑ The origin of semiconducting behavior
- ❑ Correlation of chain distribution and optical phenomena
- ❑ Morphology of thin conducting polymer films

Polymers are long chains of repeating chemical units, or monomers. They are macromolecules with a molecular weight exceeding 10,000 gm/mol.¹⁰ Their chemical skeletal structures can be linear, cyclic or branched. Polymerization of one type of monomer gives a homopolymer, while polymerization of more than one type of monomers results into a copolymer. The distribution of monomers in the polymerization of the copolymers can be statistical, random or alternating. Some polymers have semiconducting properties due to their unique structural behavior such as formation of alternating single and double bonds between the adjacent backbone carbon atoms. These conducting polymers are known as π -conjugated polymers. The semiconducting polymers have attracted considerable attention due to their wide range of applications. In this chapter, the origin of the basic electrical and optical properties of the π -conjugated polymers is briefly discussed.

2.1 The origin of semiconducting behavior

Since carbon atom (C-atom) is the main building block of most polymers, the type of bonds that its valence electrons make with other C-atoms or other elements determines the overall electronic properties of the respective polymer. Polymers can, in general, be categorized as saturated and unsaturated based on the number and type of the carbon valence electrons involved in the chemical bonding between consecutive C-atoms along the main chain of the polymers. Saturated polymers are insulators since all the four valence electrons of C-atom are used up in covalent bonds, whereas most conductive polymers have unsaturated conjugated structure. π -Conjugated polymers are excellent examples of unsaturated polymers whose electronic configuration stems from their alternate single and double carbon-carbon bonds. The fundamental source of semiconducting property of conjugated polymers originates from the overlap of the molecular orbitals formed by the

valence electrons of chemically bonded C-atoms. A neutral carbon atom has six electrons, which occupy the $1s$, $2s$ and $2p$ orbitals giving a ground state electronic configuration of $1s^2 2s^2 2p^2 (1s(\uparrow\downarrow)2s(\uparrow\downarrow)2p(\uparrow\downarrow))$. The atomic orbitals of carbon are modified into hybrid orbitals as they form covalent bonds (Figure 2.1). When a carbon atom forms a bond with another carbon atom, a $2s$ -electron is promoted to the vacant $2p$ -orbital resulting into a $2s^1 2p_x^1 2p_y^1 2p_z^1$ configuration as depicted in Figure 2.1. These electronic orbitals do not bond separately but hybridize, i.e. mix in linear combinations, to produce a set of orbitals oriented towards the corners of a regular tetrahedron. The hybrid orbitals consisting of one s orbital and three p orbitals are known as sp^3 hybrid orbitals.

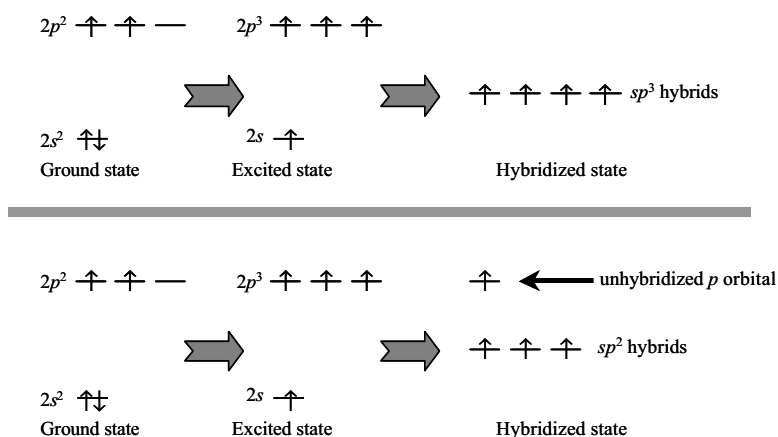


Figure 2.1 The hybridization of the valence shell electrons of a carbon atom. The upper and lower panels show sp^3 and sp^2 hybridization, respectively.

The sp^3 hybrids allow a strong degree of overlap in bond formation with another atom and this produces high bond strength and stability in the molecules. The arrangement of bonds resulting from overlap with sp^3 hybrid orbitals on adjacent atoms gives rise to the tetrahedral structure that is found in the lattice of diamond and in molecules such as ethane, C_2H_6 . In these structures all the available electrons are tied up in strong covalent bonds, named σ -bonds. Carbon compounds containing σ -bonds formed from sp^3 hybrid orbitals are termed saturated molecules. The saturated hydrocarbons, in general, have high band gaps and, hence, are classified as insulators.¹¹

Since conjugated polymers composed of alternating single and double bonds, sp^3 hybridized orbitals cannot account for their electronic structure. The alternating single and double bonds are formed from sp^2 hybrid orbitals. Mixing of one s orbital with two of the p orbitals of C-atom forms 3 sp^2 hybrid orbitals, leaving one p orbital unhybridized (See Figure 2.1). The sp^2 carbon hybrid orbitals are known to form a different bond length, strength and geometry when compared to those of the sp^3 hybridized molecular orbitals. The sp^2 hybridization has one unpaired electron (π -electron) per C-atom. The three sp^2 hybrid orbitals of a C-atom arrange themselves in three-dimensional space to attain stable configuration. The geometry that achieves this is trigonal planar geometry, where the bond angle between the sp^2 hybrid orbitals is 120° . The unmixed pure p_z orbital lies perpendicular to the plane of the three sp^2 hybrid orbitals (See Figure 2.2). The sp^2 orbitals give σ -bonds while the p_z orbitals form a different type of bonds known as π -bonds. The p_z orbitals of a polymer exhibit π -overlap, which results into a delocalization of an electron along the polymer chain. The π -bonds are, thus, considered as the basic source of transport band in the conjugated systems.^{11,12} Polyacetylene is often considered as a model conjugated polymer. It has a simple, linear structure and exhibits a degenerate ground state. Figure 2.2 illustrates the arrangement of the σ -bonds and π -bonds in polyacetylene. Owing to its structural and electronic simplicity, polyacetylene is well suited to semi-empirical calculations and has therefore played a critical role in the elucidation of the theoretical aspects of conducting polymers.¹³

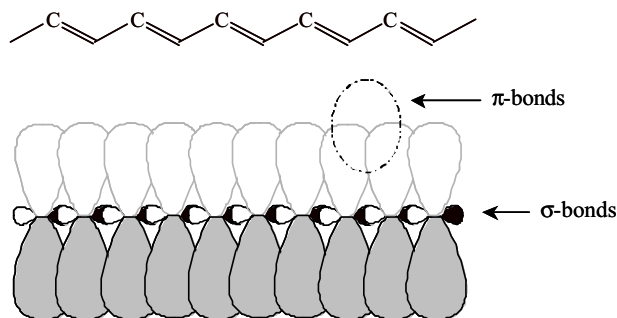


Figure 2.2 The molecular structure of polyacetylene (top), for clarity hydrogen atoms are not shown. The alternating double and single bonds indicate that the polymer is conjugated. The schematic representation of the electronic bonds in polyacetylene is depicted in the bottom panel. The p_z -orbitals overlap to form π -bonds.

In terms of an energy-band description, the σ -bonds form completely filled bands, while π -bonds would correspond to a half-filled energy band (Figure 2.3). The molecular orbitals of a polymer form a continuous energy band that lies within a certain energy range. The anti-bonding orbitals located higher in energy (π^*) form a conduction band whereas the lower energy lying bonding orbitals form the valance band. The two bands are separated by a material specific energy gap known as a *band gap* (E_g) (See Figure 2.3). The two separate bands are characterized by two quite important energy levels, namely electron affinity and ionization potential. The electron affinity of a semiconducting polymer corresponds to the lowest state of the conduction band (π^* state) or the lowest unoccupied molecular orbital (LUMO). Likewise, the ionization potential refers to the upper state of the valence band (π state) and corresponds to the highest occupied molecular orbital (HOMO). The band gap of conjugated polymers determined from optical, electrochemical and other spectroscopic measurements is within the semiconductor range of 1 to 4 eV,¹¹ which covers the whole range from infrared to ultraviolet region.

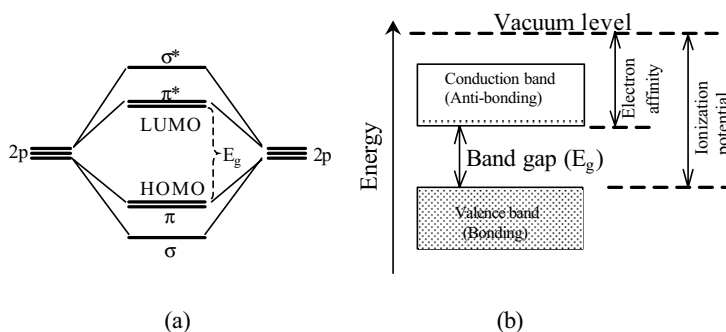


Figure 2.3 Energy level splitting of orbitals in a conjugated polymer according to a molecular orbital theory (a). HOMO, and LUMO refer to highest occupied molecular orbital and lowest unoccupied molecular orbital, respectively. Collection of molecular orbitals form bands separated by an energy gap as shown in (b).

Conjugated polymers are often considered as quasi-one dimensional metals due to the fact that the strong intrachain interaction (strong covalent bonding along the chain), and the weak van der Waals type interchain coupling interactions lead to delocalization of π -electrons along the polymer chain.¹¹⁻¹³ Every conjugated polymer has a unique chemical

structure that determines its optical and electrical behavior. The chemical structures of some π -conjugated polymers (polyacetylene, polythiophene, poly(para-phenylene-vinylene), polyfluorene) are illustrated in Figure 2.4. Polyacetylene is a classical example of conjugated polymers due to its simple and linear structure. Polythiophenes exhibit broad optical absorption and high conductivity. Substituted polythiophenes have been used to construct efficient electronic devices. Similarly, substituted poly(para-phenylene-vinylene) polymers are well studied materials due to their suitability for various applications. The polyfluorenes are well known for their high conductivity and efficient blue emission when used in light emitting devices.

The studies presented in this thesis are based on polythiophene polymers and polyfluorene copolymers that have broad absorption bands in the visible range of the solar spectrum, with an extension to near infrared absorption in the case of the polyfluorenes.

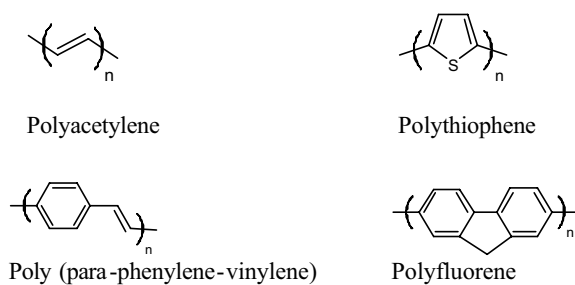


Figure 2.4 Chemical structures of some conducting π -conjugated polymers.

2.2 Correlation of chain distributions and optical phenomena

Each chain of a conjugated polymer does not stretch indefinitely but rather makes twists and coiled structures resulting into the amorphous nature of a polymer. This disordered morphology limits the delocalization length of the π -cloud of electrons to a definite length known as a *conjugation length*. This characteristic length is bounded by an energy barrier, which may be created by defects or kinks.¹³ On the other hand, the conjugation length segments have random distributions leading to different energies of the π -electrons. This is clearly manifested in the featureless, broad absorption and emission spectra of conjugated polymers (See Figure 2.5.). Assuming a simple one-dimensional particle-in-a-box picture, the longer segments will have a low π - π^* energy gap whereas the

gap of the shortest segments will be much higher. The emission spectrum is highly Stokes-shifted because excitons on high-energy segments will undergo rapid energy transfer to lower-energy segments so that nearly all the emission comes from low energy, long conjugation length segments. Chain distributions, therefore, determine the morphology, optical and electrical behavior of a conjugated polymer. The distribution of chain length can be controlled to a certain extent through well-manuevered synthesis steps.

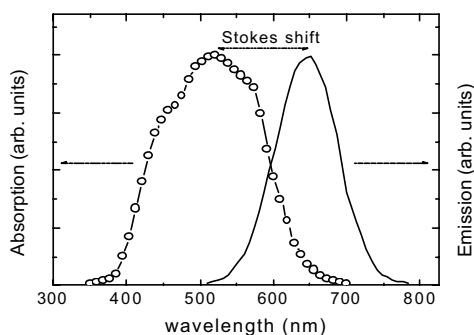


Figure 2.5 Typical schematic diagram of absorption and emission spectra of a polymer. The emission spectrum is stokes-shifted towards low energy.

2.3 Morphology of thin conducting polymer films

The main chain of conducting polymers is decorated with side chains to promote solubility in common solvents and to facilitate chain packing in solid films. Addition of side chains also reduces melting temperature, enhances flexibility and reduces intermolecular overlap of neighbouring chains. Consequently, charge transfer in polymer films is critically determined by the degree of interchain overlap or chain packing.¹⁴ Well-packed chain geometries give well-ordered crystalline phases that enhance electron delocalization length and, therefore, lead to high charge carrier mobility. The conjugated polymer poly(3-hexylthiophene), P3HT, is a classic example since it forms both amorphous and crystalline phases based on its chain conformation. Regioregular P3HT is characterized by highly packed conformation that gives ordered or crystalline phases,^{15,16} while regiorandom P3HT based solid films have amorphous phases.¹⁷ The tuning of morphology as a function of regularity in molecular structures changes both optical and electrical

profiles. For example, several orders of magnitude higher charge carrier mobility was recorded in films from regioregular P3HT as compared to its regiorandom counterpart.^{18,19}

The active layers of most polymer based electronic devices are formed by spin coating, drop casting or blade coating from common organic solvents. The degree of interchain interactions and morphology in conjugated polymer films can be controlled to some extent by monitoring chain conformations through appropriate choice of solvents, concentration of solution from which the polymer is cast, spin coating speed and thermal treatments. Specifically, the morphology of a spin-coated film is highly affected by the evaporation rate of the organic solvents.^{20,21} While high evaporation rates give highly packed films (high interchain interaction), slowly evaporating solvents lead to slow film growth rate, which is usually accompanied by formation of porous films. Polymer films with high interchain interactions are quite efficient for charge transport processes,^{18,19} but may reduce photoluminescence efficiency²² and hence have vital use in PVDs.

Morphology plays a crucial role in achieving efficient D/A based PVDs. Formation of thin films by spin coating a mixture of incompatible D/A composite from a common organic solvent often yields phase-separated domains. The boundary conditions of the bicontinuous segregated phases are further imposed by the presence of additional interfaces, such as polymer/substrate, that limits the final dimension of phase separated regions.²³ The change of morphology under various conditions is a typical characteristics of films formed from solutions. Thus, construction of efficient BHJ based solar cells requires optimum morphology that promotes dissociation of excited states and charge carrier transport.^{24,25} In summary, chain packing is a crucial element in determining solid state film morphology, which is a key factor for typical optical and electrical behaviors of polymer based electronic devices.

3. Donor/acceptor bulk heterojunction (BHJ) based solar cells

- Working principles
- The current-voltage (I-V) characteristics
- Efficiency limiting factors

Conjugated polymers have a potential to be used for conversion of solar energy into electricity. Despite the fact that conducting conjugated polymers are semiconductors their working principle in solar cells is a multi-step process, which is limited by several factors. The working principles and the factors that limit the efficiency of BHJ based PSC are discussed in the following consecutive sections. The devices considered in this chapter comprise BHJ films sandwiched between two asymmetric conducting electrodes, where the electrodes serve as anode and cathode (See Figure 3.1).

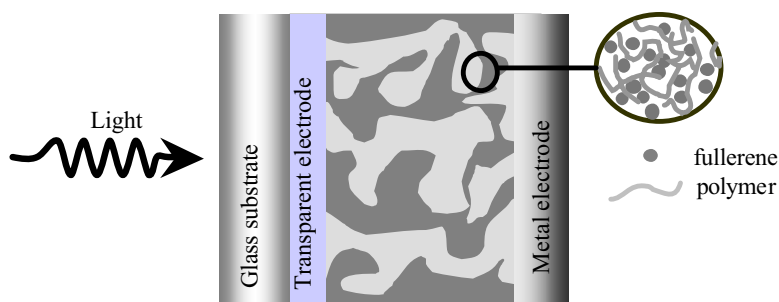


Figure 3.1 A typical schematic structure of a polymer/acceptor bulk heterojunction based solar cell. A film based on polymer/acceptor bulk heterojunction blend comprises bicontinuous phase separated regions, which are enriched by either the acceptor molecules or the electron donor polymers.

3.1 Working principles

Shining light on a PSC generates mobile excitons that have a binding energy of several tenths of electron volts.²⁶⁻²⁸ On the other hand, the diffusion length of an exciton in most conjugated polymer films is quite low (5 to 10 nm).^{29,30} This makes a bottleneck to charge generation as it leads to enormous amount of recombination within the bulk of the active layer. To achieve substantial photovoltaic effect in PSCs, excited charge pairs need

to be dissociated into free charge carriers through the assistance of electric field, bulk trap sites or interface of materials with different electron affinities. The electric field in a solar cell, in its working range, is quite low and does not dissociate excitons effectively. Other approaches have already been adopted to achieve efficient exciton dissociation.^{2,31-33} The most efficient polymer solar cells rely on BHJ active layers, which consists of blends of electron donor polymers and electron acceptor molecules. The BHJ of D/A blend composes nanoscaled heterophases that are suitable for efficient exciton dissociation. At D/A interfaces, the driving force for exciton dissociation is generated by the electrochemical potential difference between the LUMO of the donor and the LUMO of the acceptor. The electrodes collect the photogenerated free carriers; the anode (a high work function metal) collects holes and the cathode (a low work function metal) collects the electrons. The four basic steps, namely exciton creation, exciton migration, exciton dissociation and free charge carrier transfer, are depicted in Figure 3.2. Figure 3.2 is a first order-simplified illustration that does not include other relaxed states such as polaronic states.

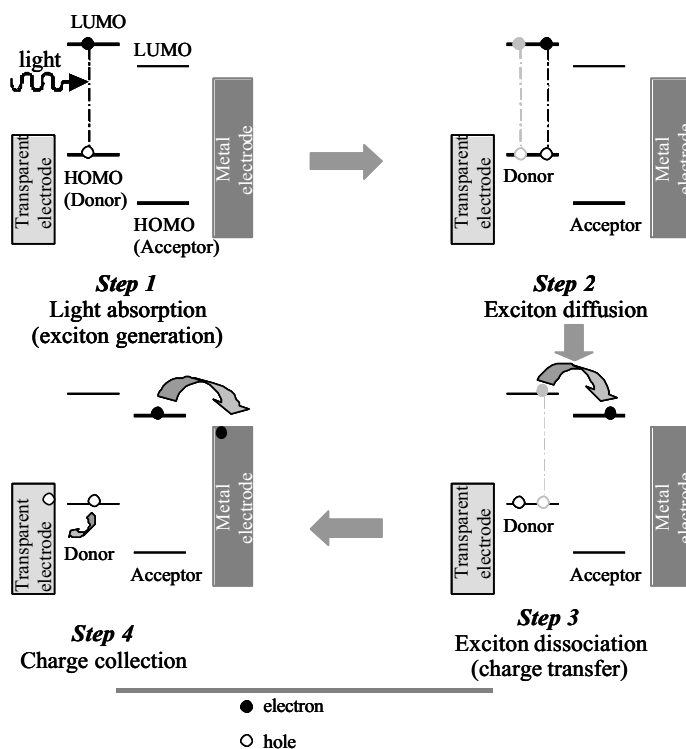


Figure 3.2 The simplified four basic steps of photocurrent generation in BHJ based solar cells. Excitons are assumed to be primarily generated in the polymers.

3.2 The current-voltage (I-V) characteristics

Typical polymer/acceptor BHJ solar cell current-voltage (I-V) characteristics measured in the dark and under white light illumination conditions are depicted in Figure 3.3. The I-V curve measured under full sun illumination (100 mW/cm^2) immediately gives several photovoltaic parameters including V_{oc} , short-circuit current density (J_{sc}), fill-factor (FF), and overall power conversion efficiency (η). Each of these parameters is shortly described in this section. The spectral response of a solar cell is also defined.

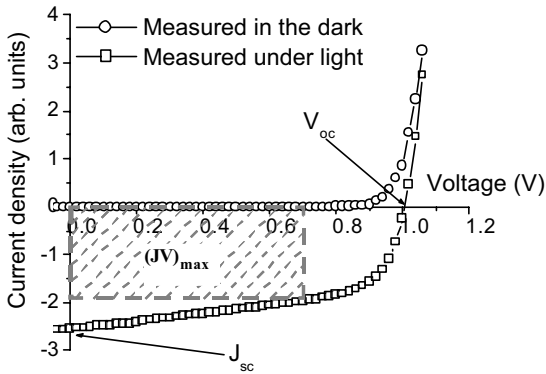


Figure 3.3 Typical current-voltage characteristics of a polymer/acceptor BHJ based solar cell. The arrows indicate the major photovoltaic parameters and the gray area defines the maximum possible power that can be extracted from the solar cell.

- (a) **The open-circuit voltage (V_{oc})** of a solar cell under light is defined as a voltage at which the net current in the cell is equal to zero. In a well behaving device, the current measured in the dark and under illumination conditions coincide for applied voltages exceeding the V_{oc} . This implies that, approximately, the V_{oc} corresponds to the net internal electric field of the device, which gives the flat band condition.
- (b) **The short-circuit current (J_{sc})** is the photogenerated current of a solar cell, which is extracted at zero applied voltage. Photocurrent is directly related to optical and electrical material properties. As observed from Figure 3.3, for an applied voltage less than V_{oc} the I-V curve recorded under illumination condition is dominated by a photo-generated current, while injection from electrodes dominates in a potential region where the applied voltage exceeds the V_{oc} .

(c) **The fill factor (FF)** of a solar cell is the measure of the power that can be extracted from the cell and is defined as

$$FF = \frac{(JV)_{\max}}{J_{sc} V_{oc}} \quad (3.1)$$

where the $(JV)_{\max}$ represents the maximum power that can be extracted from the cell. In Figure 3.3, the $(JV)_{\max}$ is defined by the area of the filled rectangle. The shape of the I-V curve is a measure of the FF; rectangular shapes give higher FF values.

(d) **The power conversion efficiency (η)** is simply the ultimate measure of the device efficiency in converting photons to electrons. Mathematically it is defined as

$$\eta = \frac{J_{sc} V_{oc}}{\mathfrak{S}_{in}} FF \quad (3.2)$$

where \mathfrak{S}_{in} accounts for the flux of light incident on the solar cell.

The I-V characteristic of a solar cell recorded under the illumination of white light does not provide detailed information on the spectral coverage and the efficiency of the device to convert monochromatic light into electrons. The short-circuit current generated at every wavelength defines the spectral response S_i of the solar cell, which is defined as

$$S_i = \frac{J_{sc,i}}{\mathfrak{S}_{in,i}} \quad (3.3)$$

where $J_{sc,i}$ is the photogenerated short-circuit current at a specific excitation wavelength λ_i and $\mathfrak{S}_{in,i}$ is the incident monochromatic photon flux. S_i is directly correlated to the external quantum efficiency (EQE) of a solar cell as

$$EQE = \frac{hc}{e} \frac{J_{sc,i}}{\mathfrak{S}_{in,i} \lambda_i} \quad \text{or} \quad EQE(\%) \approx 1240 \frac{J_{sc,i}}{\mathfrak{S}_{in,i} \lambda_i} \quad (3.4)$$

where h is Planck's constant, c is speed of light and e is an elementary charge. The second expression of equation (3.4) demands the current density, the wavelength and the photon flux to be measured in $\mu\text{A}/\text{cm}^2$, nm, and W/m^2 , respectively. EQE is sometimes referred to as an incident photon to electron conversion efficiency (IPCE). Experimentally, EQE is measured without taking care of optical losses such as light transmission through the cell and reflection away from the cell. Effective carrier generation after correction for optical losses is characterized by the so-called internal quantum efficiency (IQE).

3.3 Efficiency limiting factors

As stated previously, power conversion efficiency of a BHJ based PSC is directly correlated to the three key parameters, namely J_{sc} , V_{oc} , and FF. This means η is inherently related to material properties, device structure and interface effects.

The photocurrent (J_{sc}) of polymer solar cells is affected by several factors including generation and dissociation rates of excited states, as well as the mobility of free charge carriers. The exciton dissociation rate in BHJ films is a quite efficient process due to the availability of polymer/acceptor junctions within the range of exciton diffusion length. The method of blending conjugated polymers with high electron affinity molecules, such as C_{60} and its derivatives, has become the most efficient and rapid exciton dissociation method resulting in solar cells with high power conversion efficiencies.^{2,3,34-37} The polymer/ C_{60} interpenetrating networks give ultra fast (less than 100 fs)^{34,38,39} electron transfer rate from the optically excited polymer to C_{60} molecule. This time regime is so small that competing decay processes are extremely minimized leading to an almost complete (100%) charge transfer processes.⁴⁰ Thus, the efficiency of BHJ based solar cells is not greatly affected by exciton dissociation rates but it is rather limited by the exciton generation rate and collection efficiency of free charge carriers.

The most efficient polymer solar cells comprises P3HT for generation of excited states.³⁵⁻³⁷ However, the optical absorption of P3HT covers only the visible range of the solar spectrum, less than 700 nm, while a substantial solar energy is located in the red and infrared region. Several other conjugated polymers that have been used to construct efficient solar cells^{2,3} also have narrow optical bandwidth. Therefore, to enhance the optical absorption in solar cell materials two mechanisms can be suggested, namely utilizing thick films and/or harvesting photons in the red and near infrared portion of the solar spectrum. The first option is practically limited by the low charge carrier mobility and lifetime. The disordered nature of polymer chains forbid formation of perfect electronic wave function overlaps, which in the case of inorganic materials leads to band transport. Instead, charge carriers are highly localized and their transport is limited by the degree of the spatial and energetic disorder. Consequently, the mobility of charge carriers, in most conjugated polymers, is quite low, typically 10^{-3} to 10^{-6} cm^2/Vs .^{18,41-43} As a consequence, in thick films most of the photogenerated carriers disappear through recombination processes or forms space charges that limit flow of current. The second option, utilizing long wavelength photons, can be realized by using low band gap polymers. Such solar cells have been

demonstrated by several researchers.^{44,46} The reports have clearly demonstrated conversion of low energy photons into electrons. However, the efficiency of these new generation solar cells, in general, is quite low as compared to the high band gap polymer solar cells. This drawback may be related to the shift of the electronic levels of the polymers as a consequence of lowering band gap, which has a direct effect on the open-circuit voltage and the driving force for exciton dissociation. To draw substantial photocurrent from BHJ based solar cells, well-designed polymers that render broad optical absorption band and form well ordered chains should be considered as the best choice.

The second photovoltaic parameter that limits efficiency is the open-circuit voltage. The V_{oc} of BHJ based PSCs mainly originates from the electronic levels of the donor polymer and the acceptor molecule. In general, V_{oc} is limited by several factors including interfacial energy levels, shunt losses, interfacial dipoles and morphology of the active film. Thus, the origin of V_{oc} in BHJ based PSC is not well defined. For BHJ solar cells with ohmic contacts, V_{oc} is mainly determined by the difference between the HOMO of the donor polymer and the LUMO of the acceptor molecule indicating how much the electronic levels are crucial in determining the efficiency of such solar cells.

The third important parameter that limits efficiency is a fill factor. The direct relation of FF with current density indicates that it is greatly affected by the mobility of the charge carriers. Moreover, series resistance is also one of the limiting factors as observed in organic bilayer⁴⁷ as well as BHJ based PSCs.³⁵

The next two chapters of this thesis focus on detailed description and discussions on the V_{oc} of BHJ based solar cells and the study of charge transport in typical solar cell materials. The improvement of FF upon using better hole transporting materials will also be demonstrated.

4. The origin of open-circuit voltage in BHJ based solar cells

- Correlation of polymer electrochemical potential and the open circuit voltage of polymer/acceptor BHJ based solar cells

Efficient BHJ based PSC typically composes polymers with band gaps close to 2eV, while the V_{oc} of such devices usually falls in the range of 0.6 to 1 V.^{2,3,36} In inorganic thin film solar cells, V_{oc} is directly related to internal electric field (the MIM model), which is generated by the work function difference of the electrodes. This principle fails for PSC based on D/A interpenetrating networks. As a consequence, the origin of V_{oc} in BHJ solar cells has been an issue of debate among the scientific community.

For a solar cell with a single conjugated polymer active layer, the V_{oc} scales with the work function difference of the electrodes and thus follows the MIM model under consideration of clean polymer/electrode interfaces.⁹ Here, clean polymer/electrode interface refers to absence of dipoles or other entities that changes interface conditions, usually resulting into shift of charge injection barriers. In bilayer devices that comprise electron and hole-accepting polymers, the V_{oc} scales linearly with the work function difference of the electrodes, but with an additional contribution from the dipoles created by photoinduced charge transfer at the interface of the two polymers.⁴⁸ The V_{oc} of BHJ based solar cells is strongly correlated to inherent material properties. It was demonstrated that the open circuit voltage of polymer/fullerene BHJ based solar cells is correlated to the reduction potential of the fullerene molecule.⁸ A reduction potential defines the LUMO level of the molecule. Moreover, the V_{oc} of polymer/fullerene based solar cells is affected by the morphology of the active layer.⁹

It should be noted that in BHJ based PSCs the effect of electrodes on V_{oc} is neglected only if the cathode and anode pin to the LUMO of the acceptor molecule and the HOMO of the donor polymer, respectively (Figure 4.1).⁴⁹ In other words, the effect of electrodes is negligible only for ohmic contacts. The net electric field of such solar cells is mainly determined by the effective band gap defined by the energy difference of the LUMO of the acceptor molecule and the HOMO of the polymer. The most common anode, both for polymer based solar cells and light emitting diodes, is a transparent and thin layer

(about 100 nm) of indium thin oxide (ITO) covered with a metallic polymer, poly (3, 4 ethylene dioxythiophene)-poly (styrene sulphonate) (PEDOT: PSS). This electrode is found to make ohmic contacts with varieties of conducting polymers.⁵⁰ PEDOT:PSS is commercially available (Bayer AG and Agfa) and widely used as hole injecting (collecting) layer in polymer based solar cells and light emitting diodes. The second electrode, cathode, of polymer based diodes is commonly formed from low work function metals such as calcium and aluminum. Preferentially, for most polymer based solar cells, lithium fluoride (LiF)/aluminum (Al) evaporated thin films are used as a cathode. The presence of LiF between the active layer and Al may pin the cathode work function towards the LUMO of the acceptor material in addition to its function as a protective layer against the hot metal atoms.⁷ These typical electrodes give rise to ohmic contacts and the net internal field in such solar cells is equivalent to the difference in the electron donor HOMO and the acceptor LUMO energy levels. Thus, under light conditions, such solar cells are expected to deliver a V_{oc} equivalent to the magnitude of $e(\text{HOMO}_{donor} - \text{LUMO}_{acceptor})$, where e is an elementary charge (See Figure 4.1). Thermodynamically, this is the maximum V_{oc} the BHJ based solar cells deliver.

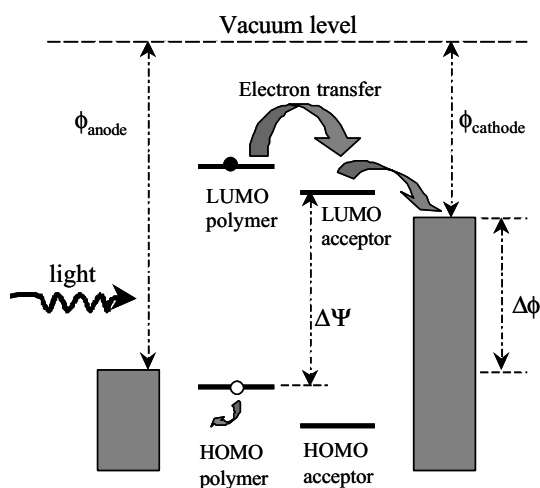


Figure 4.1 Simplified schematic showing charge carrier generation and internal fields of BHJ based solar cells under light. The V_{oc} is mainly determined by the electrochemical potential difference between the HOMO of the polymer and the LUMO of the electron acceptor molecule ($\Delta\Psi$), but under the formation of non-ohmic contacts the work function difference of the electrodes ($\Delta\phi$) also changes the V_{oc} .

The correlation of V_{oc} to polymer HOMO has become clear from the previous discussions. Accurate description of this photovoltaic parameter should, therefore, include the electrochemical oxidation potential (OP) of the polymer in addition to other relevant factors. We have investigated the correlation between the OP of a series of conjugated polythiophene polymers and the corresponding V_{oc} of solar cells comprising blends of the polythiophenes and a C_{60} derivative acceptor molecule methanofullerene [6,6]-phenyl- C_{61} -butyric acid methyl ester (PCBM) as an active layer. For this investigation, we chose six polythiophene polymers whose optical band gaps span from about 2 to 3 eV, indicating that they are optically active in the visible range of the solar spectrum.⁵¹ Moreover, to minimize the effect of processing conditions all the devices were fabricated and measured under the same conditions. The thickness and the surface morphology of the active films were approximately similar. Some of the devices employ LiF under the Al cathode while remaining group of devices relies on only Al as a cathode. Devices with LiF/Al cathode are expected to have smoother interfaces. The central result of this study is depicted in Figure 4.2, where the correlation of V_{oc} with oxidation potential of the polymers is displayed.

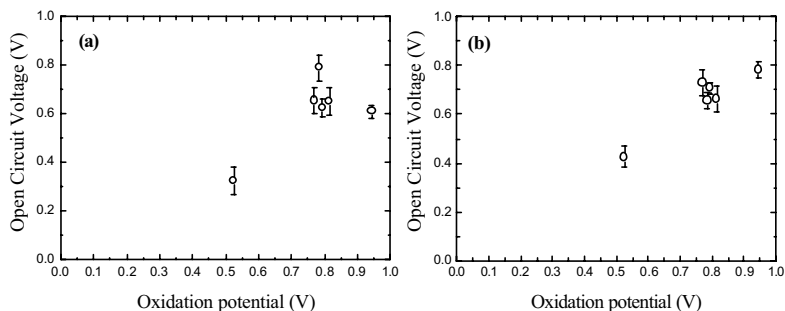


Figure 4.2 Variation of the open circuit voltage with the oxidation potential of polythiophene polymers. The data depicted in (a), and (b) refers to devices with Al and LiF/Al cathode, respectively. The open circles represent the mean value of all the measurements.

As inferred from Figure 4.2, the open circuit voltages are clearly correlated to the OP of the polythiophene polymers regardless of the cathode type. The monotonic correlation, which

has a slope close to 1 but with much scatter, shows the polymer HOMO to be a deterministic source of V_{oc} in polymer/PCBM based solar cells.

Though the choice of the polymer types and number is quite restricted, this particular study has actually shown a clear and new result that reveals a linear correlation of V_{oc} with electrochemical potential (oxidation potential) of the donor polymers. M. C. Scharber et al.⁵⁰ have recently reported a similar result that confirms an exact linearity between oxidation potential of several, various types of conjugated polymers and the V_{oc} of the corresponding polymer-PCBM BHJ solar cells. The investigation of M. C. Scharber and co-workers has involved several polymers most of which are chemically and structurally quite different from each other.

In summary, the open-circuit voltage of solar cells with polymer/acceptor active layer is clearly linearly correlated to the oxidation potential of the polymer. In particular, this linear correlation lowers the open-circuit voltage of solar cells based on low band gap polymers⁴⁴⁻⁴⁶ resulting into low power conversion efficiency. This investigation can serve as a road map in order to design and synthesis appropriate combination of conducting conjugated polymers and molecules for solar cell applications. It is, however, worth mentioning that perfect energy alignments do not set the ultimate efficiency since the optical density, charge transport and morphology also play major roles.

5. Charge carrier transport models and mobility measurement techniques

- Models of hopping transport
- Typical experimental mobility measurement techniques

Inorganic crystalline materials have well defined band transport due to the perfect overlap of their electronic wave functions. Free carriers, in such systems, are delocalized and have high mobility at room temperature. The solid-state phase of π -conjugated polymers is dominated by amorphous phases due to weak intermolecular interactions. The random distribution of conjugation length of polymer chains gives rise to distribution of electronic states, where regular lattice arrangement is lacking. Thus, a polymer film can be described as a discontinuously distributed amorphous phase, where the discontinuity is introduced by the small crystalline like ordered phases of small dimensions. The variation in molecular morphology leads to the broadening of the electronic density of states and results in hopping-type transport. The localized states put a lot of restriction on hopping transport thereby limiting the mobility of the charge carriers. Some organic systems, such as molecular crystals, form large-scale well-ordered phases that lead to substantial increase of charge carrier mobility. A brief description of hopping transport and experimental mobility measurement techniques in disordered materials, such as conjugated polymers, are discussed in this chapter.

5.1 Models of hopping transport

Hopping transport can be well approximated by a random walk, which is restricted by energetic and spatial disorders. This typical disorder controlled transport is characterized by a considerable activation energy.⁵³ Hopping transport mobility is, therefore, field and temperature dependent, where the mobility obeys the Poole-Frenkel law⁵⁴

$$\mu = \mu_0 \exp(\gamma\sqrt{E}) \quad (5.1)$$

where μ_0 is zero-field mobility, γ is field activation factor, and E is the net electric field.

Disordered systems are subjected to an energetic spread of the charge transport sites, which are often approximated in shape by a Gaussian density of states (DOS). This shape is supported by the observation of Gaussian shaped absorption spectra of polymers.⁵⁵ The shape of the DOS is important for the description of the charge transport as it reflects the disorder of the system. For disordered systems well approximated by Gaussian DOS, pioneering hopping transport model was proposed by H. Bässler.⁵⁵ This so called Gaussian disorder model (GDM) was developed through Monte Carlo simulation assuming a Gaussian distribution of transport site energy

$$\rho(\varepsilon) = (2\pi\sigma_{DOS}^2)^{-1/2} \exp\left(-\frac{\varepsilon^2}{2\sigma_{DOS}^2}\right) \quad (5.2)$$

where σ_{DOS} is the width of the Gaussian site energy distribution and the energy ε is measured relative to the center of the DOS. The Gaussian density of states is a direct manifestation of the energetic spread in the charge transporting sites of chain segments due to the fluctuation in conjugation lengths and structural disorder. Moreover, all the states within the Gaussian energy distribution are localized (Figure 5.1).

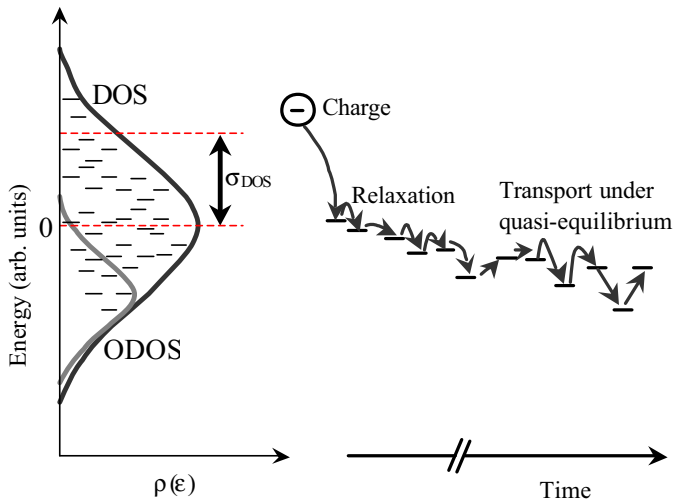


Figure 5.1 Schematic picture of hopping transport, where carriers are initially relaxed to equilibrium states and sometime excited to higher energy states through thermal stimulation. DOS represents density of states and ODOS stands for occupied density of states.

In the GDM formalism, the jump rate v_{ij} between adjacent sites i and j of energy ε_i and ε_j , respectively, and separation distance R_{ij} is the Miller-Abrahams⁵⁶ type, which is stated as

$$v_{ij} = v_0 \exp\left(-2\gamma a \frac{\Delta R_{ij}}{a}\right) \begin{cases} \exp\left(-\frac{\varepsilon_j - \varepsilon_i}{k_B T}\right), & \varepsilon_j > \varepsilon_i \\ 1, & \varepsilon_j < \varepsilon_i \end{cases} \quad (5.3)$$

In the last expression, the first exponential describes an electronic wave function overlap, while the second exponential states the Boltzmann factor for jumps upward in energy. According to this postulate, carriers that hop to sites higher in energy are thermally activated, or accelerated by a field. The effective energy barrier for hops to higher energy is equal to the energy difference between the two states. A dynamic equilibrium is reached when the effective jumps are dominated by the thermally activated hops (Figure 5.1).

In the disorder transport scheme, the field (E) and temperature (T) dependence of the mobility at equilibrium is described by⁵⁵

$$\mu_{GDM}(T, E) = \mu_0 \exp\left[-\left(\frac{2\sigma_{DOS}}{3k_B T}\right)^2\right] \begin{cases} \exp\left[C\left(\left\{\frac{\sigma_{DOS}}{k_B T}\right\}^2 - \Sigma^2\right)\sqrt{E}\right]; & \Sigma \geq 1.5 \\ \exp\left[C\left(\left\{\frac{\sigma_{DOS}}{k_B T}\right\}^2 - 2.25\right)\sqrt{E}\right]; & \Sigma < 1.5 \end{cases} \quad (5.4)$$

In equation (5.4) both the energetic and special disorder are reflected through σ_{DOS} , and Σ , respectively, whereas μ_0 is the mobility in the limit $T \rightarrow \infty$ and $E \rightarrow 0$, and C is an empirical constant that depends on site spacing. As formulated in the last equation, hopping transport in Gaussian DOS results in $\ln(\mu) \propto T^{-2}$ relationship, which deviates from the Arrhenius behavior $\ln(\mu) \propto T^{-1}$. The GDM model has been widely used to explain experimental transport studies in disordered materials, such as molecularly doped polymers,⁵⁷ molecular glasses⁵⁸ and conjugated polymers.^{59,62}

Experimental studies of charge transport in disordered systems have reproduced the Poole-Frenkel mobility behavior, $\ln(\mu) \propto \sqrt{E}$, over wide field range.⁶³⁻⁶⁵ The GDM, however, reproduces this universal law only in a narrow field range, describing experimental values only in high field range ($E \approx 10^8$ V/m).⁵⁵ To circumvent this deficiency, a new approach was suggested.^{66,67} The later scheme explicitly includes spatially correlated energetic disorder as a necessary requirement for improving the model

so as to account for the $\ln(\mu) \propto \sqrt{E}$ behavior over a broader electric field range. The spatial correlations in disordered materials may originate from long-range charge-dipole interactions. The strong coupling of phonon and electronic states in organic solids rationalizes the inclusion of correlation in transport models. For example, in conjugated polymers the presence of dipole-charge interactions has been justified due to the fact that morphological variations and an anisotropy in conjugation length distribution induce strong polarizations.⁶⁸ S. V. Novikov *et al.*⁶⁷ proposed a new empirical expression for charge mobility after performing a Monte Carlo simulation that takes care of long range charge-dipole interactions. The new correlated disorder model (CDM) is expressed as

$$\mu_{CDM} = \mu_{\infty} \exp \left[- \left(\frac{3\sigma_{DOS}}{5k_B T} \right)^2 + 0.78 \left(\left(\frac{\sigma_{DOS}}{k_B T} \right)^{3/2} - \Gamma \right) \sqrt{\frac{eaE}{\sigma_{DOS}}} \right] \quad (5.5)$$

where a is the intersite spacing between hopping sites and Γ is an empirical constant. The CDM has been used for analyzing a space charge limited (SCL) transport of conjugated polymers⁶⁵ and an electron acceptor molecule⁶⁹ sandwiched between metallic electrodes.

The disorder models, both GDM and CDM, are applicable wherever energetic disorder is dominating. However, in some systems the transport is better fitted to the Arrhenius temperature dependence $\ln(\mu) \propto T^{-1}$ rule than the disorder law $\ln(\mu) \propto T^{-2}$. If polaronic effects are taken into account, the weak temperature dependence of mobility $\ln(\mu) \propto T^{-1}$ reflects electron transfer by non-adiabatic small polaron hopping between sites with similar energies leading to a deviation from Miller-Abrahams transfer rate.⁷⁰ The later model was developed to include both polaronic and disorder effects in order to reproduce the Poole-Frenkel mobility behavior. T. Kreouzis *et al.* have successfully exploited this model to describe time-of-flight transport data of a polyfluorene conjugated polymer.⁷¹

In general, several modifications have been made to GDM in order to get better fit between experimental mobility measurements and theory. The degree of disorder in solid films is highly influenced by the morphology of the films. Thin conjugated polymer films processed from solutions are highly affected by processing conditions,³⁶ temperature treatment^{35,37,71} and the solvents used to prepare the films.^{2,9} The processing and treatment induced morphology changes are directly correlated to the amount of energetic and spatial disorders resulting in various charge transport profiles like dispersive or non-dispersive behavior. With this regard, the modifications made to GDM are quite relevant to accurately model charge transport in films that are subjected to varying degree of morphology. A review of various forms of transport models was discussed by A. B. walker *et al.*⁷²

5.2 Typical experimental mobility measurement techniques

Mobility is a key parameter as far as transport issue is concerned. In particular, the efficiency of conjugated polymer based solar cells is substantially reduced due to their low charge carrier mobility. Hence, knowledge of mobility assists designing and identifying efficient polymers for solar cell and other applications. Consequently, mobility measurement in various systems is considered as a central subject of transport studies.

Several mobility measurement methods have been developed over the last several years of research. The time-of-flight method (TOF) is one of the classical transport probing techniques that has been invoked to characterize a number of conjugated polymers.^{41,71,73,74} In this method a sheet of charge carriers generated by a short (nanosecond) light pulse drifts through the semiconductor material under an influence of an externally applied voltage. The transient time of the sheet of carriers is measured when they exit the material. The mobility of the drifting charge carriers is calculated as $\mu_{TOF} = d^2 / Ut_{tr}$, where d is the thickness of the film, U is an externally applied drift potential and t_{tr} is the transit time. The TOF method requires large film thickness (in micrometer scale), which restricts this method from measuring mobility in real thin organic active films of electronic devices. A complementary technique, which utilizes measurement of transient time for mobility measurement has emerged recently. The later method is known as charge extraction by linearly increasing voltage (CELIV).⁷⁵ In the CELIV method equilibrium carrier concentrations are extracted in such a way that carrier mobility is calculated from the time at which the extraction current reaches its maximum. In principle, this method is not limited by film thickness and it seems an appropriate method to measure mobility in thin films. However, since the amount of equilibrium carrier density in most polymeric materials is quite low, there is a restriction in using this technique for all kinds of systems. To circumvent the later problem, it is customary to generate carriers by short light pulses and extract them later. This modified method, photo-CELIVE, was found to be a more convenient method to generate and extract a large volume fraction of carriers.^{76,77}

The method of field-effect transistor (FET) is also well known technique to measure mobility in polymer based films.^{78,79} The FET mobility is calculated from the transfer characteristics of the channel current. In this method, charges are drifting along a horizontal dimension as opposed to the drift direction in devices where the active layer is sandwiched between conducting electrodes. This conduction principle, together with high charge concentration in the channel, usually gives high carrier mobility values that in most cases

cannot be realized in diodes. The origin of high FET mobility value was recently attributed to carrier density dependent mobility.^{80,81}

The other rather common method of measuring mobility in sandwich-structured devices is the space charge limited model (SCLM). The principle of this model is quite simple; charge injection into the bulk of a polymer film and I-V characteristics measurements are simultaneously performed. This technique does not describe transient phenomena since it is static in its nature. The SCLM⁸² is used to fit the SCL portion of the I-V curve thereby delivering mobility values. This method has successfully been used to investigate the field and temperature dependence of hole mobility in conjugated polymers^{65,83} and an electron acceptor molecule.⁶⁹ The later method can probe transport of charge carrier in solar cells and light emitting diodes that comprise thin films. This method will further be emphasized in the next chapter.

6. The method of space charge limited current

- ❑ Extraction of transport parameters from I-V characteristics
- ❑ Carrier transport study using unipolar sandwich structure devices
- ❑ Bipolar transport in pristine acceptor molecules

As discussed in the previous chapter, several charge probing techniques have been developed over years. Each method has its own merits and drawbacks when applied for studies of charge carrier transport in thin films of disordered materials. In this chapter, the method of space charge limited model is considered for extraction of transport parameters from I-V characteristics of unipolar sandwich structure devices. This method enables to probe charge carrier transport in a solar cell or a light emitting diode.

6.1 Extraction of transport parameters from I-V characteristics

In PSC, charge carriers either photogenerated or injected into the bulk of the active layer have to reach the electrodes through the mechanism of diffusion, drift or both. These various charge transport mechanisms can be identified and explained in terms of device and semiconductor material parameters. In this section, the various features of typical I-V characteristics of polymer-based diodes, measured in the dark, will be discussed briefly. The bulk-limited transport, which is mainly influenced by materials property, is discussed in detail.

6.1.1 Typical features of I-V characteristics measured in the dark

The I-V characteristic of a diode, measured under dark conditions, has several features that correspond to various types of charge transport within the device (Figure 6.1). Under forward bias conditions the I-V plot of a polymer based diode with asymmetric electrodes reveals typically three main transport features.

- a) **The low bias regime** : This region is characterized by an ohmic flow of charges formulated as $J \propto \frac{V}{d}$, where J is the current density, V is the applied bias potential and d is the thickness of the active semiconductor layer. Injection of charge carriers from the electrode(s) into the semiconductor material is quite reduced due to the low bias voltage, which cannot compensate for the internal field. The current flow originates mainly from extrinsic effects that give leakage currents.
- b) **Intermediate bias regime** : Increasing the bias voltage further decreases an internal electric field thereby enhancing injection of charge carriers from electrodes into the bulk of the semiconductor. A sharp slope usually characterizes the injection-limited (IL) region and the current increases exponentially with bias voltage. The IL conduction is commonly described either by Fowler–Nordheim tunneling injection⁸⁴ or by Richardson–Schottky thermionic emission.⁸⁵ Owing to the amorphous nature of organic materials and the presence of defects at interfaces, the classical metal-to-organic injection models described previously may not be always true. This has been demonstrated both experimentally⁸⁶ and in Monte Carlo simulations,⁸⁷ where injection phenomena is best described by a hopping injection

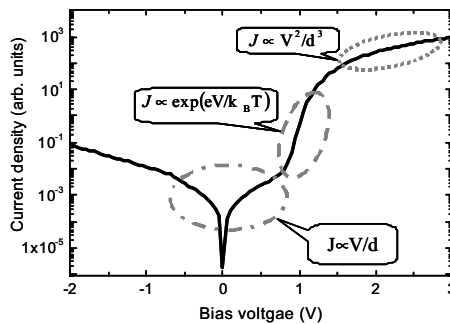


Figure 6.1: Various features of a typical I-V characteristic of a polymer based diode. Under forward bias conditions, the ohmic region ($J \propto V/d$), injection-limited region ($J \propto \exp(eV/k_B T)$), and the space charge limited region ($J \propto V^2/d^3$) are clearly displayed. Here, J is current density, V is potential, d is film thickness, T is temperature, k_B is the Boltzmann constant and e is the elementary charge.

into a random organic dielectric. In general, IL region is governed by the factors related to the semiconductor/metal interface. The injection barrier, which is often controlled by the interface dipoles, fermi level alignments and defects, is the main factor that controls the injection process. On the other hand, in certain cases the image force also plays a role-giving rise to current backflow.⁸⁸ The energetic disorder introduced by the roughness at organic/metal interface may also contribute to the modification of injection barriers.⁹⁹ Detailed knowledge of injection processes in devices based on metalorganic-metal structures is quite important for various applications such as light emitting diodes. The detailed analysis is, however, beyond the scope of this thesis.

- c) **The high bias regime** : After the bias voltage compensates for the built-in potential of a diode (flat band condition), current injection becomes enormous. However, due to low charge carrier mobility as well as the presence of traps, the outflow rate of the injected carriers is reduced greatly and charges accumulate in the bulk of the semiconducting organic layer. The transport flow is now dominantly controlled by the space charge limited current (SCLC) resulting into saturation of current as inferred from Figure 6.1.^{60,82} The transport of carriers in the SCLC region can be modeled in order to estimate carrier mobility and other transport parameters. Detailed discussions of the SCL model will be given in the next chapters.

In the presence of deep traps the transport profile is modified, the modifications being reflected in the change of the slopes of the I-V curve. One typical feature of a diode I-V curve is its rectification due to the fact that the reverse voltage current is considerably smaller under the absence of localized leakage current paths.

6.1.2 Formulation of space charge limited current model

Simulation of charge carrier transport in polymer-based devices is one of the major issues to be addressed in order to understand efficiency-limiting factors in PSCs. Despite the fact that in polymer films pure band transport is suppressed, the traditional charge transport laws, which were originally derived for inorganic materials, can still be applicable for organic materials as well. In this section formulation of SCLC model is described starting from basic transport equations.

PSC and light emitting devices comprise thin (nano scaled) films of the active material. Consequently, charge transport in polymer-based diodes is often simplified as a one-dimensional process. In this context, the basic transport equations describing charge transport behavior are the one dimensional Poisson's and continuity equations for electrons and holes. In particular, if the effects of traps are negligibly small, the drift-diffusion current equations and the Poisson's equation, respectively, are given by⁸²

$$J_n = e \left(-\mu_n(x) n(x) \frac{d\psi}{dx} + D_n \frac{dn}{dx} \right) \quad (6.1)$$

$$J_p = e \left(-\mu_p(x) p(x) \frac{d\psi}{dx} - D_p \frac{dp}{dx} \right) \quad (6.2)$$

$$\frac{dE(x)}{dx} = \frac{e}{\epsilon} (p(x) - n(x)) \quad (6.3)$$

where J_n (J_p) is the electron (hole) current density, $n(x)$ ($p(x)$) is the electron (hole) density, D_n (D_p) is electron (hole) diffusion constant, μ_e (μ_p) is the electron (hole) mobility and ϵ is equal to $\epsilon_0 \epsilon_r$, with ϵ_0 the permittivity of free space and ϵ_r the relative dielectric constant of the semiconductor. The electric field strength $E(x)$ is related to the electrostatic potential $\psi(x)$ as $E(x) = -\frac{d\psi}{dx}$. The mobility and diffusion coefficients are related through the Einstein relation $D = \mu k_B T$, where k_B is Boltzmann's constant and T is temperature. Under the condition of SCL transport, the drift current dominates the net current flow and the diffusion part is often neglected.

Analytical expression of SCLC can be derived for a constant mobility and drift dominated transport. Under the assumption of an absence of traps, or negligible trap density, solving the current equation together with the Poisson equation gives an analytical solution

$$J_{SCL} = \frac{9}{8} \epsilon \mu \frac{V^2}{d^3} \quad (6.4)$$

where μ is the charge carrier mobility and d is the film thickness. Equation (6.4) describes a trap free SCL transport, often known as the Mott-Gurney square law, trap free square law and Child's law for solids.⁸² When traps are present, most of the injected holes (electrons) are localized and do not contribute to current flow. In such cases, the dependence of current on voltage is determined by the density and energy distribution of the trap sites. Inclusion of single discrete traps into the analysis of the SCL current leads to

$J \propto V^2/d^3$, while in the presence of traps with exponential trap distribution the SCLC takes a power law dependence of the form $J \propto V^{k+1}/d^{2k+1}$ where k is defined in terms of a characteristic trap distribution constant.^{42,82,90}

6.2 Carrier transport study using unipolar sandwich structure devices

The SCLM enables one to selectively study a single carrier transport in a solar cell or light emitting diode. The freedom of having a single type of carrier in a device is adjusted by the choice of electrodes. In this section, practical examples of hole transport in solar cell materials using unipolar devices is presented and discussed.

6.2.1 The concept of single carrier devices

Experimentally, it is possible to construct unipolar sandwich structured devices that give either electron dominated or hole dominated current flow. Both, the so-called electron only devices (EoD) and hole only devices (HoD) can be constructed by tuning charge injection barriers through appropriate choice of electrodes. Literally, the electrodes of EoD should line up with the LUMO level of the semiconductor in order to discriminate hole

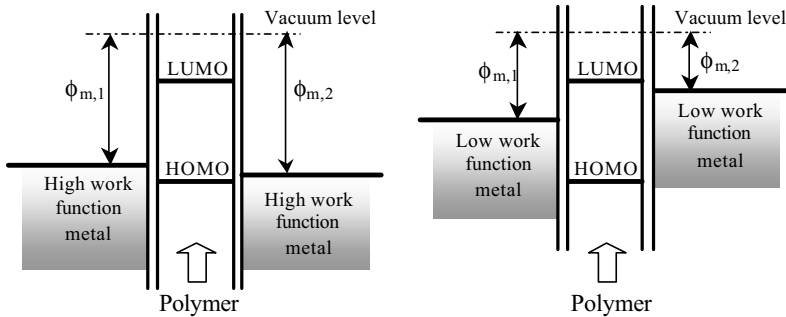


Figure 6.2. The geometry of hole only (left), and electron only (right) sandwich structured devices. The schematic diagram is shown for the case where the electrodes are not in contact with the polymer film. $\phi_{m,1}$ and $\phi_{m,2}$ represent the work functions of the two metal electrodes.

injection. The best choices of such ohmic electrodes are low work function metals such as calcium (Ca), magnesium (Mg), aluminum (Al) and the like. On the contrary, high work

function metals such as gold (Au) and palladium (Pd) can well behave as hole injectors and hence serve in constructing HoDs. Here it is worth mentioning that the suggestion for using a given metal for forming an ohmic electrode, while discriminating injection of one type of carrier, is not without complications. Some metals are well known for forming dipoles at the polymer/metal interface thereby shifting the injection barrier for the otherwise unwanted charge carrier.

Accumulation of charges in a bulk of a polymer film creates a field that reduces current flow. The net effect is the transition of constant mobility to field dependent mobility of the Poole-Frenkel type. Under this circumstance, the experimental SCL I-V characteristic is analyzed by solving the relevant current equations and Poisson's equation together with the Poole-Frenkel mobility equation. Due to the field dependence of mobility, however, exact analytic solution cannot be obtained, which leads us to make numerical calculations. This method has been utilized to investigate hole transport,^{65,83} as well as electron transport⁶⁹ in thin polymer films sandwiched between coplanar electrodes. In this thesis, we have used the SCLM to investigate hole transport in series of polyfluorene copolymers and their blends with electron acceptor molecules.

6.2.2 Hole transport in alternating polyfluorene copolymers (APFO)

The APFO (Alternating PolyFluOrene) family of copolymers are based on a fluorene monomer combined with donor-acceptor-donor (D-A-D) co-monomers and designed to have a low band gap and form birefringent liquid crystalline phases (See Figure 6.3).^{3,91} These copolymers have been used to construct efficient solar cells.^{3,46,92} Some of

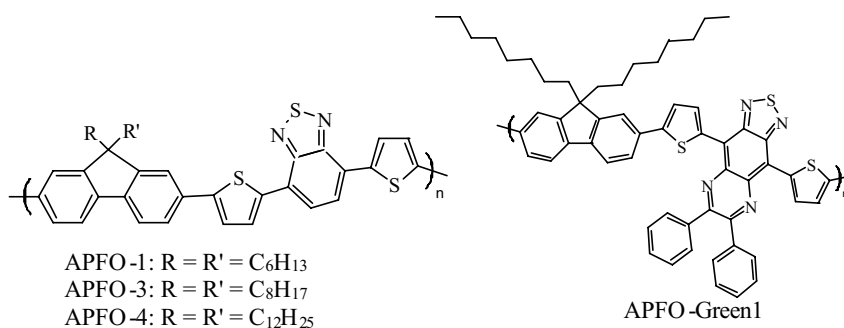


Figure 6.3. The Chemical structures of low band gap polyfluorene copolymers (APFOs).

these copolymers have broad absorption band that extends into the red and near infrared solar spectrum. The low band gap APFOs have been used to construct solar cells that generate photocurrent in the near infrared region.^{44,93,94} The field and temperature dependent hole mobility studies were performed for series of polyfluorene copolymers poly(2,7-(9,9-dihexyl-fluorene)-*alt*-5,5-(4',7'-di-2-thienyl-2',1',3'-benzothiadiazole))

(**APFO-1**), poly(2,7-(9,9-dioctyl-fluorene)-*alt*-5,5-(4',7'-di-2-thienyl-2',1',3'-benzothiadiazole)) (**APFO-3**), poly(2,7-(9,9-didodecyl-fluorene)-*alt*-5,5-(4',7'-di-2-thienyl-2',1',3'-benzothiadiazole)) (**APFO-4**) and poly(2,7-(9,9-dioctyl-fluorene)-*alt*-5,5-(4',9'-di-2-thienyl-6',7'-diphenyl-[1',2',5']thiadiazolo-[3',4'-g]quinoxaline)) (**APFO-Green1**) (Figure 6.3).

Hole transport in APFOs is field and temperature dependent, which is a typical feature of hopping transport. The I-V characteristics of single carrier devices have at most symmetric shapes, confirming formation of ohmic electrodes at both interfaces (Figure 6.4). Charge carrier (hole) mobility (Figure 6.5) and field activation factor are determined by fitting the experimental data by numerically solving the transport equations (Equations, 5.1, 6.2 and 6.3). Further analysis of the experimental data is performed using the Gaussian disorder model, more relevantly the CDM. The later analysis enables to estimate the energetic and spatial disorders through the knowledge of the width of the Gaussian site energy distribution (σ_{DOS}) and the average hopping distance (a).

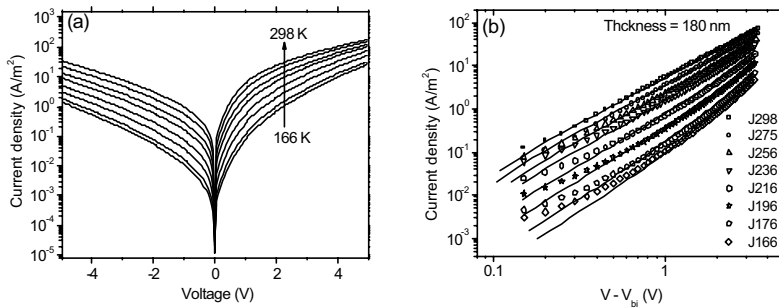


Figure 6.4. A typical temperature dependent current-voltage characteristics of ITO/PEDOT:PSS/APFO-Green1/Au hole only diode: (a) experimental data, and (b) experimental data (symbols) together with the numerically simulated data (lines).

The comparative studies enable to understand the variation of hole transport as a function of material structure. For example, APFO-1, APFO-3 and APFO-4 have the same aromatic backbone structures while their alkyl side chains have different lengths. Commonly, the main chain of polymers is decorated with side chains for various reasons. Side chains may play a crucial role in determining the conformation and solvent processability of conjugated polymers⁹⁵. It is well understood that long, non-branched hydrocarbon chains can easily pack together and form well ordered solution-processed films.⁹⁶ Therefore, the

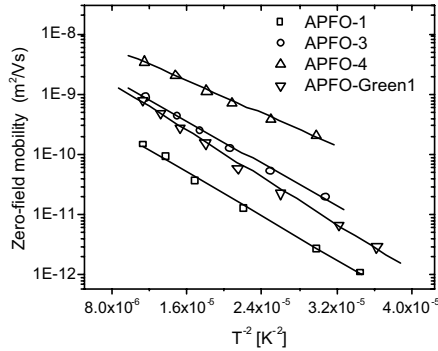


Figure 6.5: The variation of hole mobility as a function of temperature. The mobility values are extracted from experimental current-voltage curves of hole only devices.

Table 6.1. Summary of hole transport parameters as a function of copolymer type. The values are extracted from experimentally measured I-V characteristics of hole only diodes.

Polymer name	mobility (μ_0)* (m^2/Vs)	field activation factor (γ)* (m/V) ^{1/2}	Intersite distance (a)* (nm)	Width of DOS (σ_{DOS})* (meV)
APFO-1	$(1.5 \pm 1) \times 10^{-10}$	$(5.6 \pm 0.2) \times 10^{-4}$	1.90 ± 0.2	69 ± 4
APFO-3	$(9 \pm 1) \times 10^{-10}$	$(3.2 \pm 0.2) \times 10^{-4}$	1.55 ± 0.2	64 ± 4
APFO-4	$(3.4 \pm 1) \times 10^{-9}$	$(2.5 \pm 0.2) \times 10^{-4}$	1.50 ± 0.2	57 ± 4
APFO-Green1	$(8 \pm 0.4) \times 10^{-10}$	$(8.8 \pm 0.2) \times 10^{-5}$	1.95 ± 0.02	70 ± 1

* Room temperature values.

alteration of molecular conformation as a function of structural change has a direct link with the charge carrier localized hopping processes. Measurement of mobility in FET and hole only diodes based on symmetric and asymmetric poly(p-phenylene vinylene) (PPV)⁹⁷ polymers has shown a clear relationship between side chain length and charge transport. However, such comparative studies can only be made under similar processing conditions.⁹⁷ The comparative study of hole transport in APFOs indicates that energetic disorder is more pronounced than spatial disorder (See Table 6.1). The origin of this disorder is mainly attributed to structural changes.

To further analyze the link between structural change and charge transport, systematic photovoltaic study was performed on solar cells with polymer/fullerene BHJ active films.⁹⁸ The optically active part (electron donors) of the BHJ film was varied while PCBM was used as an electron accepting and transporting material. We have exclusively selected APFO-3 and APFO-4, which differ only by their side chain length. As shown earlier, APFO-4 is a better hole transporting material as compared to APFO-3 (Figure 6.5 and Table 6.1). Moreover, since the two polymers have different alkyl side chains, blending them with PCBM, for solar cell application, is accompanied by varying morphology in solid films. Comparative studies have shown that the structurally induced morphological and transport differences are revealed in variation of the efficiency of the corresponding solar cells.⁹⁸ Significant difference was recorded in the fill factor values; APFO-4 based solar cells render higher FF than that of APFO-3 based solar cells. The later observation is well correlated to the basic fact that FF is most likely limited by the mobility of the charge carriers. Therefore, the tuning of FF (Table 6.1, and Figure 6.6) with polymer type is consistent with the transport studies. While APFO-3 based solar cells give higher current, because its miscibility with PCBM is better due to its shorter side chains, APFO-4 based devices have rendered better FF mainly because the photogenerated holes are effectively transported to anode.

Based on the previous results, one may think of using blends of the two polymers in the same device in order to exploit their best properties. Here it is assumed severe thermodynamically driven phase separations are suppressed due to the structural and chemical similarities of the polymers. Indeed, solar cells with APFO-3/APFO-4/PCBM active layers have made significant changes in photovoltaic output as compared to devices that rely on thin films of APFO-3/PCBM and APFO-4/PCBM blend films. The change in FF values is quite significant as displayed in Figure 6.6, which is attributed to improved

hole transport. The overall power conversion efficiency was also enhanced by about 15%.⁹⁸

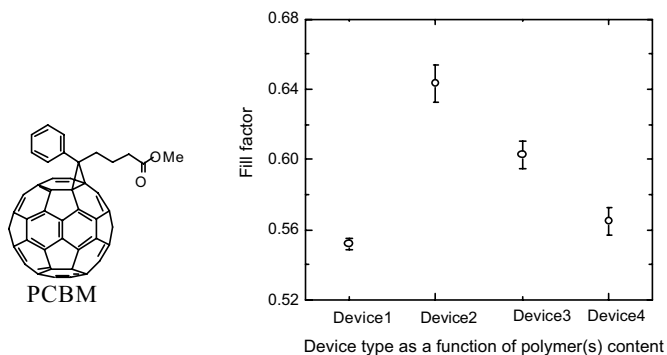


Figure 6.6. The chemical structure of PCBM (left) and the fill factor values (right) as a function of solar cell type. The electron donor polymers are APFO-3 (Device 1), APFO-4 (Device 2), APFO-3:APFO-4 (1:1, wt.%) (Device 3), and APFO-3:APFO-4 (3:1, wt.%) (Device 4). All the devices comprise 80% (by wt.) PCBM.

In summary, the studies presented in this section are good examples to demonstrate the interplay between polymer chemical structure, morphology and charge transport. Chemical structures that give well-ordered morphology are favourable from transport point of view. However, for polymer/molecule based solar cells, nano scale phase separation is the necessary condition for efficient charge generation. Thus, fabrication of polymer-based solar cells with competitive efficiency demands the optimisation of molecular structures of polymers as well as electron acceptor molecules, with the aim of enhancing morphology, charge generation and transport in the polymer/acceptor bicontinuous heterojunction films. This basic issue will remain the main focus of chemists and device physicist in order to fabricate next generation efficient polymer based solar cells.

6.2.3 Hole transport in blends of APFOs and acceptor molecules

In BHJ of D/A solar cell materials, morphology is a key parameter that affects exciton dissociation and the transport of free charge carriers. Dissociation of excitons demands a close proximity of the donor and acceptor moieties while continuous material

networks give rise to good percolation paths. Concurrently, the interplay between the driving force for exciton dissociation and polymer LUMO (band gap) is so crucial that varying polymer type demands an appropriate electron acceptor material. This has clearly been demonstrated for solar cells with low band gap electron donor copolymers.^{44,93,94} As far as transport is concerned, well-mixed D/A materials create well-behaved transport percolation paths. Thus, adequate driving force at D/A interface (i.e. adequate energy offset between the LUMO of polymer and the LUMO of acceptor) cannot be taken as the necessary and sufficient condition to construct efficient BHJ based solar cells. The knowledge of the charge carrier transport in the D/A blend layer is the central issue to be addressed in order to understand and tackle efficiency limiting mechanisms in BHJ based PSCs.

Hole transport in D/A heterojunction films is greatly influenced by the structural and chemical behaviors of the constituent elements. As a result of low entropy of mixing, spin coated films of polymer/fullerene thin films are accompanied by phase separation processes.⁹⁸⁻¹⁰⁰ Small scale phase separations create favorable conditions for efficient photogeneration of charge carriers and their subsequent collection towards electrodes. In D/A blend films, holes and electrons are supposed to transit in the pure polymer and acceptor phases, respectively. Accordingly, hole mobility measured in pure polymer film and in blend films are expected to have the same magnitude. The same should hold for electron mobility. However, this simple assumption does not seem to hold in real devices. For various types of polymer/PCBM BHJ films hole mobility in the blend phase has substantial increase over values measured in pure polymer films. This has clearly been demonstrated in TOF,^{101,102} solar cell^{103,104} and FET¹⁰⁵ measurements. Poly (3-hexylthiophene) is a well-studied conjugated polymer. The state of the art polymer solar cells with efficiencies ranging from 4 to 5% rely on P3HT/PCBM BHJ active films.^{35,36,106} Unlike for several other polymers, the room temperature hole mobility in P3HT/PCBM (50:50- wt.%) based solar cell is about three orders of magnitude less than its values measured in pure P3HT films.¹⁰⁷ However, it was shown that hole mobility in the pure polymer and blend films attain the same value upon annealing the blend film.¹⁰⁷ This radical change of transport is directly correlated to change in morphology of the blend films.

The change of hole mobility as a function of acceptor loading has also been detected in APFO-Green1/PCBM¹⁰⁸ and APFO-3/PCBM¹⁰⁹ BHJ films. In both types of blends, in general, hole mobility is enhanced in the presence of high concentration of

PCBM in the blend. However, hole mobility in APFO-Green1/PCBM device attains a local maximum at about 67 % (wt.) of PCBM content, whereas in APFO-3/PCBM device hole mobility increases monotonically with increasing PCBM content (Figure 6.7). The local peak observed in Figure 6.7 (a) is followed by a sharp decrease in hole mobility. The reason for breaking of hole percolation path beyond PCBM concentration of 67 % is not clear yet. However, it appears that more interconnected domains, enriched with either of the materials, are formed at PCBM concentration of about 67% and above. While increasing PCBM concentration obviously enhances connection of the PCBM rich domains (enhancing electron percolation path), the polymer rich domains might further be separated from each other thereby suppressing hole transport. On the other hand, the monotonic increment of mobility in APFO-3/PCBM BHJ layers reflects a better interaction between the APFO-3 and PCBM leading to smooth morphology.

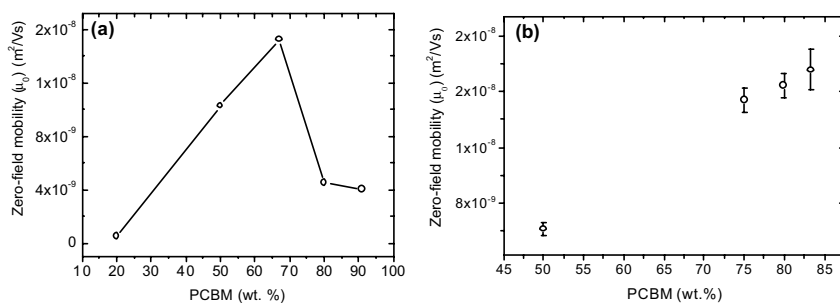


Figure 6.7. Variation of hole transport in hole dominated diodes with an active layer of APFO-Green1:PCBM, (a) and APFO-3:PCBM, (b). The content of PCBM is varied.

Further investigations were performed by replacing PCBM with a new class of C_{70} derivative electron acceptor molecule, 3'-(3,5-Bis-trifluoromethylphenyl)-1'-(4-nitrophenyl)pyrazolino[70]fullerene (BTPF70). This molecule provides relatively better driving force for exciton dissociation when blended with low band gap polyfluorene copolymers, whose absorption spectrum is extended into the near infrared (typically APFO-Green1).^{44,94} Mixing any amount of BTPF70 with APFO-Green1 decreases hole transport in the blend phase (Figure 6.8), which makes BTPF70 non-attractive as compared to PCBM. Similar trend was observed when APFO-3 is blended with this molecule.¹⁰⁵ This particular molecule has three isomers, which have similar electrochemical behaviors in

solution. The degradation of hole mobility as a function of BTPF70 loading may be taken as a direct manifestation of morphology changes.

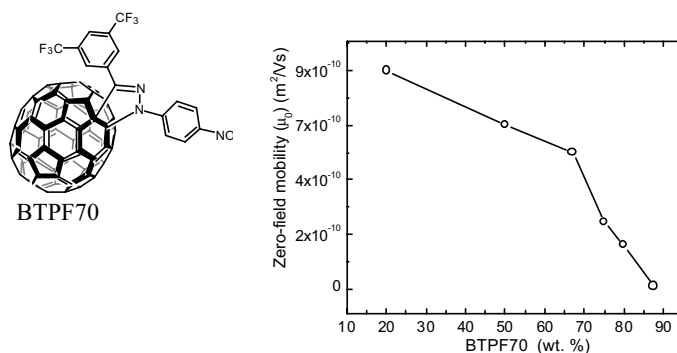


Figure 6.8. The molecular structure of BTPF70 (left) and the variation of hole transport in APFO-Green1:BTPF70 hole only diodes (right).

It is noted that the BHJ film is characterized by a varying morphology due to non-perfect mixing of the two components. Moreover, the phase-separated islands may be subjected to varying dielectric media due to the difference in their material contents. Such differences may polarize the surroundings, which may contribute to the varying transport profiles. Thus, the change of hole transport as a function of acceptor loading should be attributed to the collective effect of all the local interactions within the BHJ blend film. It can also be argued that hole transfer from a polymer to acceptor may take place under favourable energetic conditions, a process that might lead to a completely new hole transport path. The later concept is briefly discussed in the next chapter based on experimental evidences.

6.3 Bipolar transport in pristine acceptor molecules and its implication for charge carrier transport in polymer/acceptor BHJ based solar cells

The fullerene molecules, PCBM and BTPF70, are the building blocks of D/A based organic solar cells. Their major contribution to photocurrent generation is two fold: enhancing exciton dissociation and participating in charge transport. It was demonstrated that hole transport in D/A mixed phase is greatly influenced by acceptor type and concentration. In films where APFO-3 and APFO-Green1 were mixed with PCBM, hole transport was generally enhanced as compared to the values extracted from pristine

polymer films. In this chapter, the bipolar transport in acceptor films will be demonstrated. Its implication for the enhancement of hole transport in polymer/acceptor blends is suggested.

Studies of bipolar transport in acceptor materials can to some extent deliver information about the peculiarities observed in the change of hole transport in the polymer/acceptor phases described in the previous sections. In order to observe correlations between bipolar transport in acceptor molecules and hole transport in BHJ based films, we have built and characterized light emitting devices with acceptor active layers. Such devices can be considered as the most relevant devices to deliver good understanding of bipolar transport in a given material. The structure of a LED is similar to that of solar cell while it operates in an opposite way to solar cells. In a LED holes and electrons are injected into the active layer and later gives rise to light if the injected charges recombine radiatively.

The acceptor bipolar devices were constructed in such a way that the hole injecting electrode was varied from ITO to ITO/PEDOT:PSS, while the cathode was a thermally evaporated LF/Al layer.^{108,111} Since the HOMO levels of both molecules are large (≈ 6.1 eV),¹⁰⁸ the hole injection barrier at both ITO and ITO/PEDOT:PSS is large given the work function of ITO and PEDOT:PSS of ≈ 4.7 eV, and 5.1 eV, respectively. Assuming no Fermi level pinning at the anode, light emission from the LEDs is either not possible or takes place at substantially large onset potential. It was observed that devices with ITO anode are not emissive while LEDs with ITO/PEDOT:PSS anode emit light at a considerably small bias voltage, about 1V (Figure 6.9). The emission of light at quite low bias voltage is quite remarkable. In organic LEDs, the injection barrier at organic/electrode interface is a complicated function of several parameters. Specifically, the formation of thin dipole layers at organic semiconductor/electrode interface is a well-known process that results into shifting of charge injection barriers.^{112,113} This effect cannot be ruled out for PEDOT:PSS/BTPF70 and PEDOT:PSS/PCBM interfaces though no direct evidence is available yet.

Both acceptors allow bipolar transport, as confirmed through the light emission process. The studies indicate that the molecules, PCBM and BTPF70, may transport holes as well as electrons when used in solar cells. This could partially account for hole mobility enhancement in most polymer/PCBM blend films as a function of PCBM loading.¹⁰¹⁻¹⁰⁵ Several mechanisms can be suggested for the observed enhancement of hole mobility in the

presence of an acceptor molecule. The first contribution to the improvement of hole transport, upon the presence of PCBM, may originate from increased interchain interactions, or increased conjugation length, within the blend layer. However, for some systems, hole mobility is much greater in the blend phase than in the pure polymer film^{101, 104,105,108,109} suggesting that changes in morphology alone may not account for dramatic hole mobility increments. Here we are referring to the pristine films, which have not gone

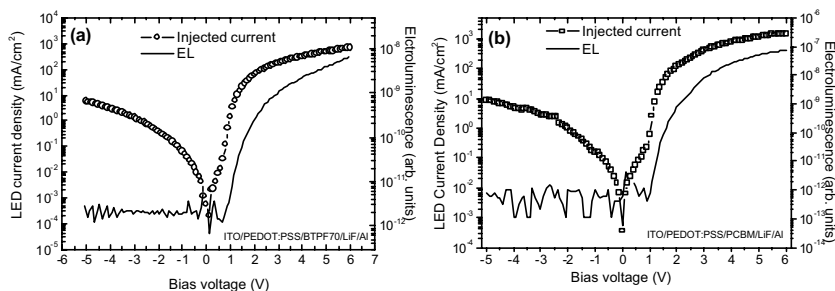


Figure 6.9. The injected current density, and electroluminescence of (a) ITO/PEDOT:PSS/BTPF70/LiF/Al, and (b) ITO/PEDOT:PSS/PCBM/LiF/Al light emitting diodes.

through any form of treatment. Thus, the second option is a creation of a new and faster percolation path possibly through the acceptor phase. PCBM is known to conduct holes better than most of the conducting conjugated polymers.¹¹⁰ The second option demands hole transfer from polymer to PCBM under the close proximity of the HOMOs of the donor and acceptor materials. The last assertion follows from the assumption that most of the holes are photogenerated in the polymer phase for a solar cell under light. The participation of PCBM in hole transport, in solar cell, can be exemplified based on the work of C. M Björström *et al.* They have investigated the vertical distribution of materials in APFO-3/PCBM BHJ films using the method of dynamic secondary ion mass spectroscopy.¹¹⁴ They have demonstrated that while PCBM tends to segregate towards the bottom substrate (ITO/PEDOT:PSS), the polymer was found to move towards the free surface. The APFO-3/PCBM blend film is a rather good active layer for solar cells, delivering efficiency exceeding 2%³⁹ in spite of an expected reduced hole collection due to a reduced amount of polymer layer at the anode. We suggest that in solar cells with APFO-3/PCBM active layer

the segregated PCBM promotes hole conduction resulting into increased hole collection efficiency and the overall solar cell power conversion efficiency.

The correlation between bipolar transport in acceptor and hole mobility enhancement is not true for polymer/BTPF70 BHJ films since a decrease in hole conduction is observed as compared to hole mobility measured in the pure polymer films.^{105,108} We suggest that the reduction of hole transport in polymer/BTPF70 layers is in direct proportion to unfavourable morphological changes and little or no hole transfer from polymer to BTPF70. The reported electron mobility in pure PCBM film is in the order of 10^{-2} to 10^{-3} cm^2/Vs ,^{69,101,1110} while that of BTPF70 is in the order of 10^5 cm^2/Vs .¹⁰⁸ The low electron mobility in BTPF70 can also be taken as a limiting factor for achieving reduced hole transport in polymer/BTPF70 blends. The low electron mobility can be taken as a signature of more disorder that leads to build up of SCL conditions and/or increase in recombination.

To sum up, The SCLM has been successfully used to describe hole mobility in both pure polymer and polymer/fullerene blend layers. Hole mobility depends on the structure of the materials indicating the crucial effect of morphology on charge transport. In polymer/PCBM blend films, hole transport is enhanced as compared to hole mobility in pure polymer films. The later was attributed to morphological changes as well as formation of other percolation paths, mainly hole conduction through the acceptor layer. The BTPF70 gives rise to reduction of hole mobility in polymer/BTPF70 blend. Thus, different acceptors obviously provides different exciton dissociation energy and charge transport profiles. The knowledge of charge transport in solar cell materials is quite beneficial in order to select the appropriate polymer-molecule combinations that provides excellent charge generation and collection efficiencies.

7. Transparent polymer cathode: towards all-polymer solar cells

□ Vapor phase polymerized thin and transparent PEDOT layers serve as electron conductors (cathode) for photovoltaic devices

Organic solar cells are promising because of their simple and low-cost construction steps as compared to the complicated and expensive procedures used to fabricate inorganic solar cells. As most conjugated polymers are soluble in common solvents, inexpensive liquid-based processing techniques create the possibility of making large area, low weight and flexible solar cells. Traditional polymer based solar cells are constructed in the form of sandwich structures (See Figure 3.1), where the active layer is confined between two conducting metallic electrodes. Further reduction of cost can be achieved by replacing the metallic electrodes by cheap and easily processable polymer electrodes.

It is customary to use transparent polymer hole conducting buffer layers in polymer solar cells and light emitting diodes.^{2,3,8,36,92,115} In particular, PEDOT:PSS has become a universal hole conducting layer in polymer based solar cells and light emitting diodes. The chemical structures of PEDOT and PSS are depicted in Figure 7.1.

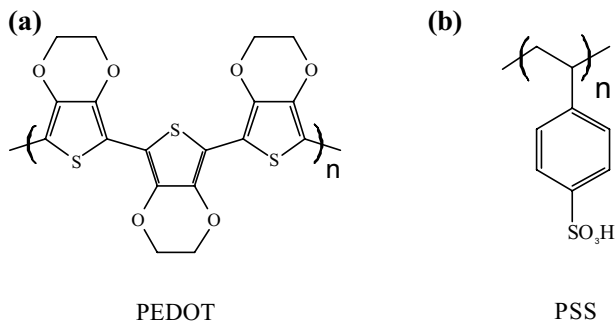


Figure 7.1 The chemical structure of PEDOT (a), and PSS (b).

To use bare PEDOT:PSS layer as a hole conductor, its conductivity and sheet resistance should be improved significantly. Mixing the commercially available PEDOT-

PSS with a sorbitol is known to change the conductivity of the resulting thin films, with typical conductivity values as high as 48 S/cm.¹¹⁶ Similarly, blending PEDOT:PSS with a polyethylene oxide¹¹⁷ or other secondary dopants like dimethyl sulfoxide, N,N'-dimethyl formamide, tetrahydrofuran and 2,2'-thiodiethanol also improves the conductivity of PEDOT:PSS significantly, with typical values reaching about 100 S/cm.^{118,119} We have previously demonstrated solar cells that utilize PEDOT:PSS buffer layers with varying conductivity.¹²⁰ Vapor-phase polymerization (VPP) technique has become a more elegant approach to achieve highly conducting PEDOT layers. The VPP synthesis route allows direct synthesis of pure PEDOT (with out PSS) solid films on a substrate. The thin films obtained by this method are transparent and remarkably conductive; conductivities as high as 1000 S/cm have been achieved.¹²¹ Using this method, prototype solar cells with vapor-phase polymerized PEDOT (VPP-PEDOT) anode and an Al cathode have been demonstrated.^{122,123} These polymer electrodes, having excellent conductivity, can be used to fabricate cheap, flexible and large area polymer based electronic devices.

Development of an all-plastic solar cell can lead to a substantial cost reduction in the future photovoltaic market. However, construction of efficient and all-plastic solar cells is challenging due to the limited choice of electrode materials. PEDOT:PSS can be considered as one of the electrodes (anode) if its sheet resistance is reduced and its conductivity is enhanced by doping or other means. Then the most difficult step is to find an organic material that serves as an electron-conducting layer (cathode). We have recently demonstrated VPP-PEDOT as a potential candidate for a cathode in photovoltaic devices.¹²⁴ The VPP-PEDOT has a low work function (4.3 ± 0.1 eV) as measured by an ultraviolet photoelectron spectroscopy (Figure 7.2). This value is close to that of most low work function metals such as aluminum and silver. The low work function of this material was also confirmed based on comparative photovoltaic studies made on solar cells that uses VPP-PEDOT and PEDOT:PSS as buffer layers on top of an ITO bottom electrode, whereas the top electrodes are kept the same. Typical IV curves recorded under white light illumination are depicted in Figure 7.3. The difference in work function of the two forms of PEDOT resulted into variation of the photovoltaic output of the solar cells. In particular, the solar cells have shown substantial differences in the values of their open-circuit voltages due to the difference in the charge injection barrier at the polymer/bottom electrode interfaces. This comparative photovoltaic study also indicates that the work function of VPP-PEDOT is small so that the hole injection barrier at the polymer/VPP-

PEDOT is larger resulting into reduction of the V_{oc} and the J_{sc} . Thus, VPP-PEDOT's low work function and modest conductivity makes this material a potential candidate as an electron conducting layer.

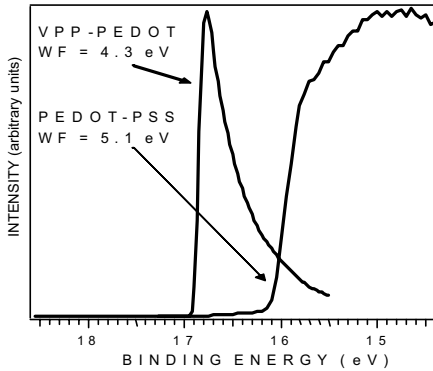


Figure 7.2 The secondary-electron cutoff of ultraviolet photoelectron spectroscopy (UPS) spectra from which the work function (WF) of VPP-PEDOT and PEDOT:PSS is determined.

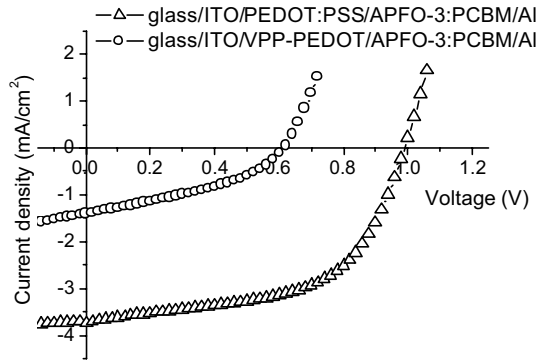


Figure 7.3 The current-voltage (I-V) characteristics of glass/ITO/VPP-PEDOT/APFO-3:PCBM/Al (open circles) and glass/ITO/PEDOT:PSS/APFO-3:PCBM/Al (open triangles) under white light illumination (A.M. 1.5, 100 mW/cm²).

Traditionally, the upper electrode (cathode) of a polymer-based diode is formed by vacuum deposition of low work function metals like aluminum (Al) and calcium (Ca) on

top of the active layer. Replacing metallic cathodes of diodes with VPP-PEDOT demands placing thin layer of this conducting polymer on top of an active semiconductor layer. Direct polymerization of VPP-PEDOT on an active, say, solar cell material is not permitted due to the fact that the polymerization steps demand coating of catalysts on top of the active layer. Therefore, other ways should be sought to integrate this material into sandwiched structured devices. The method of inverted diodes and lamination can be considered as alternative possibilities. The inverted diode method refers to construction of a diode in a reverse order where the active film is coated on the cathode (VPP-PEDOT) and the anode is formed on top of the active layer. Inverted solar cells that comprise thin films of PEDOT:PSS, capped with thin metal strips, have previously been demonstrated.¹²⁵ The draw back of this method is that the PEDOT:PSS does not easily adhere to polymer films. Moreover, doping PEDOT:PSS with various dopants such as sorbitol requires a heat treatment at an elevated temperature. This cannot be done after the PEDOT:PSS is formed on top of the active organic film since thermal treatments can alter the optical and electrical behaviors of the organic film. The second option is to use a lamination technique. Traditional lamination methods are performed under elevated temperatures, which cannot be employed for polymer based electronic devices for the reasons stated earlier. However, soft contact lamination technique (SCLT) is a good candidate here. The later method exploits the good adhesion property of soft elastomeric materials put in conformal contact with smooth surfaces. That means a VPP-PEDOT synthesized on an elastomeric substrate can be laminated with an active layer, which is prepared on a separate substrate (See Figure 7.4). The two parts are simply put in conformal contact without applying any pressure or heat treatments. The elastomer acts as 'glue' and keeps the two parts together where finally the Van der Waals bonding forces generate the sticking forces between the PEDOT and active layer.

We have employed the SCLT and constructed prototype solar cells with VPP-PEDOT cathode and ITO/PEDOT:PSS anode. The SCLT has previously been effectively used to construct organic transistors¹²⁶ as well as organic light emitting diodes that generate uniform and stable light.¹²⁷⁻¹²⁹ The laminated solar cells with VPP-PEDOT cathode have inferior performance as compared to their counterparts with metal cathodes.¹²⁴ The low performance is not the main issue here since our aim is to demonstrate functional solar cells with transparent polymer electrode. The main challenge here is to synthesize a uniform, and smooth VPP-PEDOT layer that enhances its adhesion to the active layer. In general, the construction steps should be performed in a dry and clean environment in order to avoid

various contaminations including dust and moisture. The results indicate that further improvement is necessary to enhance the performance of the laminated devices. The fabricated solar cells are considered as first prototypes for all-plastic and transparent solar cells. The soft lamination together with the use of the low work function transparent plastic electrode, such as VPP-PEDOT, can also open a route to go towards low-cost multi-layer and tandem solar cells.

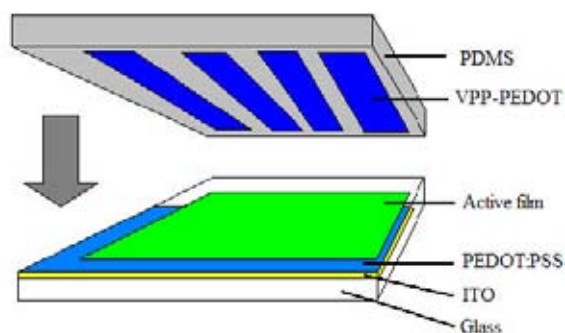


Figure 7.4 Schematic illustrations of the top and bottom components of the prototype solar cells with VPP-PEDOT cathode. Laminating the two parts together completes the solar cell.

In summary, VPP-PEDOT can be employed as an electron conducting layer in electronic devices. If its conductivity is improved further and its sheet resistance is reduced, VPP-PEDOT can replace metallic electron conductors. Its work function can align with the electron affinity of low band gap polymers such as APFO-Green1 when used in diodes.

8. Polarized light emission from APFOs

□ Aligned liquid crystalline phases of the polyfluorene copolymers for application in polarized light emitting diodes

Polymers have inherited a lot of interesting and unique properties that makes them useful for various applications. A good example is a chain orientation phenomenon, which is well known in forming optical anisotropy. In this context, liquid crystalline (LC) polymers can be taken as examples of materials that show orientation under various conditions. Thin films of a LC polymer held under elevated temperature undergo phase transitions, commonly revealing various types of phases that are characterized by different degree of orientations. Above the glass transition temperature (T_g), the polymer turns into a relaxed state and upon further heating results into the so-called isotropic liquid phase characterized by high optical transparency and lack of long range ordering. The melt can be converted into ordered phases upon cooling. Among the different organizations that are contained in the LC state of a polymer, the nematic LC phase (Figure 8.1, and Figure 8.2) is unique since it involves long range ordering. This phase can directly be formed from the isotropic melt.

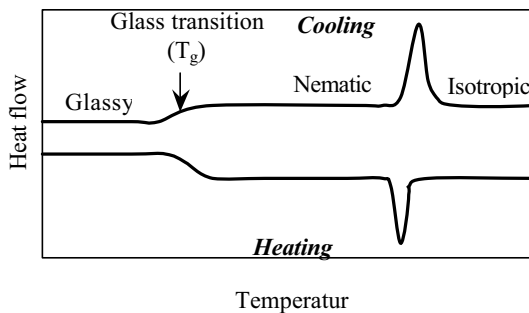


Figure 8.1 Schematic of differential scanning calorimetry (DSC) thermograph of a polymer. The lower curve shows the phase shift trace under heating conditions while the upper shows the reverse.

Liquid crystalline phase of a semiconductor thin film is characterized by strong dipoles, which are pointing along a common axis (director) and hence experiences unique optical behavior, such as birefringence, when heated above T_g (Figure 8.2). Thermally induced optical selectivity, namely emission and absorption of polarized light, is the main feature of LC materials that makes them quite attractive for use in display and other relevant devices.

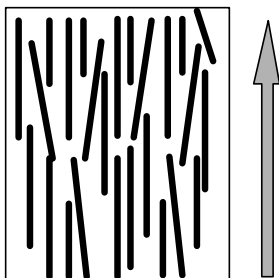


Figure 8.2 Schematic of nematic liquid crystalline structure with the director indicated by the arrow. This phase has a long range ordering.

The polyfluorene copolymers APFO-3 and APFO-Green1 inherits LC phase and undergo phase transitions at elevated temperatures. In this chapter the formation of LC state in thin solid films of these copolymers will be described. As an application, polarized light emitting diodes are demonstrated.

To use LC materials in optical or electrical devices, unidirectional orientations are quite important in order to induce uniform optical/electrical characteristics. It is a common practice to grow films in a nematic phase and keep the ordering permanently. Conventional methods employ the so-called alignment layer (AL) so that the LC layer grows epitaxially from the surface of the alignment layer.¹³⁰⁻¹³² An AL is either patterned through lithographic methods¹³³ or mechanically rubbed¹³² to form a template that initiates a uniaxial growth of the LC state in thin organic films. Polyamide^{134,135} is a classical alignment layer while other conducting polymers such as poly(p-phenylenevinylene)¹³⁶ and PEDOT:PSS^{137,138} have also been used to align LC polymers.

Solid films of APFO-3 and APFO-Green1 show birefringence when heated up at high temperatures. Both polymers turn into transparent melt phase above a temperature of 170° C. The LC phases of both polymers have been permanently oriented by the use of a

rubbed PEDOT:PSS layer. The aligned polymer layers are optically active as observed under crossed polarizers (Figure 8.3).



Figure 8.3 Birefringence observed under an optical microscope equipped with crossed polarizers. The colored monographs were recorded at a 45° angle difference with the dark ones.

The preference of PEDOT:PSS over other ALs is due to the fact that it serves as a hole injector (anode) for light emitting diodes, which were later constructed by using the thermally converted polymer films. The absorption (Figure 8.4) and photoluminescence of the aligned films have shown dichroic changes when measured parallel and perpendicular to the rubbing direction. The dichroic ratios calculated at the maximum of the absorption spectrum varies from 3 to 5 for both copolymers.¹³⁹

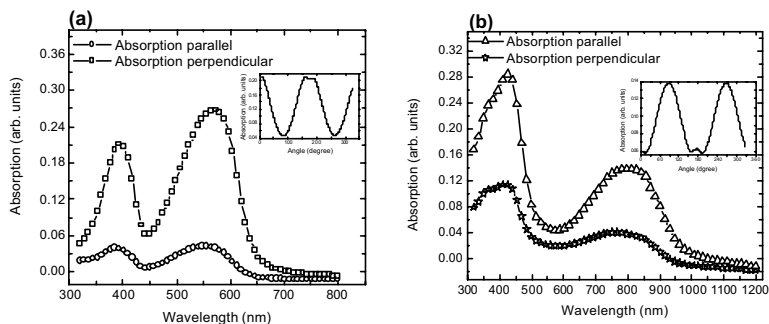


Figure 8.4 Typical absorption spectrum of the aligned layers of APFO-3 (a), and APFO-Green1 (b) solid films. The absorption measurements were done by placing a polarizer between the sample and the incident light. The insets show the peak absorption as a function of scanning angle of the polarizer.

With the aim of producing polarized light, we have fabricated and characterized LEDs based on aligned films of the APFOs. We chose to use PEDOT:PSS as an alignment layer because of its additional functionality as a hole injector.¹³⁹ The LEDs with an active layer of aligned films emit polarized light at an onset voltage close to 2V. In spite of the damaged PEDOT:PSS bottom layer through the rubbing process, this onset potential is not terribly large. Similar to the absorption dichroism, the EL spectra also show dichroism, with dichroic ratio at the peak wavelength ranging from 5 to 11 for APFO-3 and 3 to 5 for APFO-Green 1 based diodes. The LEDs emit quite broad-spectrum, covering the red and near infrared and their peak EL emissions are located at about 950 nm for APFO-Green1, and 660 for APFO-3.

These materials are quite interesting due their application both for photovoltaic and light emitting diodes. The results presented in this section suggest that the APFOs could be developed for use in display devices and other applications. The direct use of a polarized backlight without polarizer requires high polarization (dichroic) ratios, between 10 and 200, depending on applications.¹³² It has been demonstrated that, under well controlled fabrication and measurement conditions, the EL peak dichroic ratio of well-aligned polyfluorene polymers spin coated on a PEDOT:PSS alignment layer reaches up to 31.¹³⁸ The primitive mechanical rubbing (by hand) we have performed in this study has given rise to non-uniform alignment and damage of the hole injector PEDOT:PSS layer. Polarised electroluminescent light sources in the near and mid-infrared are not common; one of the few is based on electroluminescent carbon nanotubes.¹⁴⁰ Applications for such light sources are even less developed. A conceivable use might be in optical sensors operating in the infrared wavelength range, where molecular fingerprint could be accessible and where optical waveguide sensors therefore might be appropriate for chemical sensing. Incoupling of IR light into waveguides, or excitation of plasmons in near field optical configurations, might be of relevance for such sensors.

By and large, this study has enabled us to make use of the LC phase of the polyfluorene copolymers to produce polarized light in the red and infrared light spectrum. These materials can be developed into sensors and display devices by optimising processing conditions such as forming well-ordered templates using a rubbing machine and making heat treatments in an inert environment to avoid oxidation. It is also interesting to investigate the charge transport in aligned films both in diode and transistor configurations in a well-controlled fashion. Since the materials are oriented, the transport parallel and

perpendicular to the direction of orientation could be easily detected. Thus, such studies are useful to understand structure-charge transport correlation.

References

1. C. K. Chiang, C. R. Fincher, Y. W. Park, A. J. Heeger, H. Shirakawa, E. J. Louis, S. C. Gau, and A. G. MacDiarmid, *Electrical Conductivity in Doped Polyacetylene*, Phys. Rev. Lett. **39**, 1098-1101 (1977).
2. S. E. Shaheen, C. J. Brabec, N. S. Sariciftci, F. Padinger, T. Fromherz, and J. C. Hummelen, *2.5% efficient organic plastic solar cells*, Appl. Phys. Lett. **78**, 841-843 (2001).
3. M. Svensson, F. Zhang, S. C. Veenstra, W. J. H. Verhees, J. C. Hummelen, J. M. Kroon, O. Inganäs, and M. R. Andersson, *High performance polymer solar cells of an alternating polyfluorene copolymer and a fullerene derivative*, Adv. Mater. **15**, 988-991 (2003).
4. Z. Bao, A. Dodabalapur and A. J. Lovinger, *Soluble and processable regioregular poly(3-hexylthiophene) for thin film field-effect transistor applications with high mobility*, Appl. Phys. Lett. **69**, 4108-4110 (1996).
5. E. J. Meijer, D. M. De Leeuw, S. Setayesh, E. Van Veenendaal, B.-H. Huisman, P. W. M. Blom, J. C. Hummelen, U. Scherf, J. Kadom, and T. M. Klapwijk, *Solution-processed ambipolar organic field-effect transistors and inverters*, Nat. Mater. **2**, 678-682 (2003).
6. R. H. Friend, R. W. Gymer, A. B. Holmes, J. H. Burroughes, R. N. Marks, C. Taliani, D. D. C. Bradley, D. A. Dos Santos, J. L. Brédas, M. Logdlund, and W. R. Salaneck, *Electroluminescence in conjugated polymers*, Nature **397**, 121-128 (1999).
7. C. J. Brabec, S. E. Shaheen, C. Winder, and N. S. Sariciftci, *Effect of LiF/metal electrodes on the performance of plastic solar cells*, Appl. Phys. Lett. **80**, 1288-1290 (2002).
8. C. J. Brabec, A. Cravino, D. Meissner, N. S. Sariciftci, T. Fromherz, M. T. Rispen, L. Sanchez, and J. C. Hummelen, *Origin of the open circuit voltage of plastic solar cells*, Adv. Funct. Mater. **11**, 374-380 (2001).
9. J. Liu, Y. Shi, and Y. Yang, *Solvation-induced morphology effects on the performance of polymer-based photovoltaic devices*, Adv. Funct. Mater. **11**, 420-424 (2001).
10. P. W. Atkins, *The elements of physical chemistry*, Oxford University Press (1992).
11. W. R. Salaneck, R. H. Friend, and J. L. Brédas, *Electronic structure of conjugated polymers: Consequences of electron-lattice coupling*, Phys. Rep. -Rev. Sec. Phys. Lett. **319**, 231-251 (1999).
12. A. J. Heeger, Nobel lecture: *Semiconducting and metallic polymers: The fourth generation of polymeric materials*, Rev. Mod. Phys. **73**, 681-700 (2001).
13. A. J. Heeger, S. Kivelson, J. R. Schrieffer, and W.-P. Su, *Solitons in conducting polymers*, Rev. Mod. Phys. **60**, 781-850 (1988).
14. B. J. Schwartz, *Conjugated polymers as molecular materials: How chain conformation and film morphology influence energy transfer and interchain interactions*, Annu. Rev. Phys. Chem. **54**, 141-172 (2003).
15. E. M.-Osteritz, A. Meyer, Bea M. W. Langeveld-Voss, René A. J. Janssen, E. W. Meijer, and P. Bäuerle, *Two-dimensional crystals of poly(3-Alkylthiophene): Direct visualization of polymer folds in submolecular resolution*, Angew. Chem. Int. Ed. **39**, 2679-2684 (2000).
16. P. J. Brown, H. Sirringhaus, M. Harrison, M. Shkunov, and R. H. Friend, *Optical spectroscopy of field-induced charge in self-organized high mobility poly(3-hexylthiophene)*, Phys. Rev. B **63**, 125204(1)- 125204 (11) (2001).

17. S. Hugger, R. Thomann, T. Heinzel, and T. Thurn-Albrecht, *Semicyrystalline morphology in thin films of poly(3-hexylthiophene)*, *Colloid Polym. Sci.* **282**, 932–938 (2004).
18. Z. Bao, A. Dodabalapur, and A. J. Lovinger, *Soluble and processable regioregular poly(3-hexylthiophene) for thin film field-effect transistor applications with high mobility*, *Appl. Phys. Lett.* **69**, 4108-4110 (1996).
19. H. Sirringhaus, N. Tessler, and R. H. Friend, *Integrated optoelectronic devices based on conjugated polymers*, *Science* **280**, 1741-1744 (1998).
20. Y. Shi, J. Liu, and Y. Yang, *Device performance and polymer morphology in polymer light emitting diodes: The control of thin film morphology and device quantum efficiency*, *J. Appl. Phys.* **87**, 4254-4263 (2000).
21. T.-Q. Nguyen, R. C. Kwong, M. E. Thompson, and B. J. Schwartz, *Improving the performance of conjugated polymer-based devices by control of interchain interactions and polymer film morphology*, *Appl. Phys. Lett.* **76**, 2454-2456 (2000).
22. B. Xu, and S. Holdcroft, *Molecular control of luminescence from poly(3-hexylthiophenes)*, *Macromolecules* **26**, 4457-4460 (1993).
23. A. C. Arias, N. Corcoran, M. Banach, R. H. Friend, and J. D. MacKenzie, *Vertically segregated polymer-blend photovoltaic thin-film structures through surface-mediated solution processing*, *Appl. Phys. Lett.* **80**, 1695-1697 (2002).
24. F. Zhang, K. G. Jespersen, C. Björström, M. Svensson, M. R. Andersson, V. Sundström, K. Magnusson, E. Moons, A. Yartsev, and O. Inganäs, *Influence of solvent mixing on the morphology and performance of solar cells based on polyfluorene copolymer/fullerene blends*, *Adv. Funct. Mater.* **16**, 667–674 (2006).
25. W. Geens, S. E. Shaheen, B. Wessling, C. J. Brabec, J. Poortmans, and N. S. Sariciftci, *Dependence of field-effect hole mobility of PPV-based polymer films on the spin-casting solvent*, *Org. Electron.* **3**, 105–110 (2002).
26. R. N. Marks, J. J. M. Halls, , D. D. C. Bradley, R. H. Friend, and A. B. Holmes, *The photovoltaic response in poly(p-phenylene vinylene) thin-film devices*, *J. Phys.: Condens. Matter.* **6**, 1379-1394 (1994).
27. C. H. Lee, G. Yu, D. Moses, and A. J. Heeger, *Picosecond transient photoconductivity in poly(p-phenylenevinylene)*, *Phys. Rev. B* **49**, 2396-2407 (1994).
28. J.-W. van der Horst, P. A. Bobbert, M. A. J. Michels, and H. Bässler, *Calculation of excitonic properties of conjugated polymers using the Bethe–Salpeter equation*, *J. Chem. Phys.* **114**, 6950-6957 (2001).
29. M. Theander, A. Yartsev, D. Zigmantas, W. Mammo, M. R. Andersson, and O. Inganäs, *Photoluminescence quenching at a polythiophene/C₆₀ heterojunction*, *Phys. Rev. B* **61**, 12957-12963 (2000).
30. D. E. Markov, C. Tanase, P. W. M. Blom, and J. Wildeman, *Simultaneous enhancement of charge transport and exciton diffusion in poly(p-phenylene vinylene) derivatives*, *Phys. Rev. B* **72**, 045217 8 (1)-045217 (6) (2005).
31. L. Chen, D. Godovsky, O. Inganäs, J. C. Hummelen, René A. J. Janssen, M. Svensson, and M. R. Anderson, *Polymer photovoltaic devices from stratified multilayers of donor-acceptor blends*, *Adv. Mater.* **12**, 1367-1370 (2000).
32. J. J. M. Halls, C. A. Walsh, N. C. Greenham, E. A. Marseglia, R. H. Friend, S. C. Moratti, A. B. Holmes, *Efficient photodiodes from interpenetrating polymer networks*, *Nature* **376**, 498-500 (1995).
33. G. Yu, and A. J. Heeger, *Charge separation and photovoltaic conversion in polymer composites with internal donor/acceptor heterojunctions*, *J. Appl. Phys.* **78**, 4510-4515 (1995).

34. N. S. Sariciftci, L. Smilowitz, A. J. Heeger, F. Wuld, *Photoinduced electron transfer from a conducting polymer to Buckminsterfullerene*, *Science* **258**, 1474-1476 (1992).
35. W. Ma, C. Yang, X. Gong, K. Lee, and A. J. Heeger, *Thermally stable, efficient polymer solar cells with nanoscale control of the interpenetrating network morphology*, *Adv. Funct. Mater.* **15**, 1617-1622 (2005).
36. G. Li, V. Shrotriya, J. Huang, Y. Yao, T. Moriarty, K. Emery, and Y. Yang, *High-efficiency solution processable polymer photovoltaic cells by self-organization of polymer blends*, *Nat. Mater.* **4**, 864-868 (2005).
37. M. R.-Reyes, K. Kim, and D. L. Carrolla, *High-efficiency photovoltaic devices based on annealed poly(3-hexylthiophene) and 1-(3-methoxycarbonyl)-propyl-1-phenyl-(6,6) C₆₁ blends*, *Appl. Phys. Lett.* **87**, 083506(1)- 083506(3) (2005).
38. C. J. Brabec, G. Zerza, G. Cerullo, S. De Silvestri, S. Luzzatti, J. C. Hummelen, and N. S. Sariciftci, *Tracing photoinduced electron transfer process in conjugated polymer/fullerene bulk heterojunctions in real time*, *Chem. Phys. Lett.* **340**, 232-236 (2001).
39. G. Zerza, C. J. Brabec, G. Cerullo, S. De Silvestri, and N. S. Sariciftci, *Ultrafast charge transfer in conjugated polymer-fullerene composites*, *Synth. Met.* **119**, 637-638 (2001).
40. P. Schilinsky, C. Waldauf, and C. J. Brabec, *Recombination and loss analysis in polythiophene based bulk heterojunction photodetectors*, *Appl. Phys. Lett.* **81**, 3885-3887 (2002).
41. H. Antoniadis, M. A. Abkowitz, and B. R. Hsieh, *Carrier deep-trapping mobility-lifetime products in poly(p-phenylene vinylene)*, *Appl. Phys. Lett.* **65**, 2030-2032 (1994).
42. R. Pacios, J. Nelson, D. D. C. Bradley, and C. J. Brabec, *Composition dependence of electron and hole transport in polyfluorene:[6,6]-phenyl C₆₁-butyric acid methyl ester blend films*, *Appl. Phys. Lett.* **83**, 4764-4766(2003).
43. M. Redecker, D. D. C. Bradley, M. Inbasekaran, and E. P. Woo, *Nondispersive hole transport in an electroluminescent polyfluorene*, *Appl. Phys. Lett.* **73**, 1565-1567 (1998).
44. X. Wang, E. Perzon, F. Oswald, F. Langa, S. Admassie, M. R. Andersson, and O. Inganäs, *Enhanced photocurrent spectral response in low-bandgap polyfluorene and C₇₀-derivative-based solar cells*, *Adv. Funct. Mater.* **15**, 1665-1670 (2005).
45. M. M. Wienk, Mathieu G. R. Turbiez, M. P. Struijk, M. Fonrodona, and René A. J. Janssen, *Low-band gap poly(di-2-thienylthienopyrazine):fullerene solar cells*, *Appl. Phys. Lett.* **88**, 153511(1)- 153511(3) (2006).
46. F. Zhang, E. Perzon, X. Wang, W. Mammo, Mats R. Andersson, and O. Inganäs, *Polymer solar cells based on a low-bandgap fluorene copolymer and a fullerene derivative with photocurrent extended to 850 nm*, *Adv. Funct. Mater.* **15**, 745-750 (2005).
47. J. Xue, S. Uchida, B. P. Rand, and S. R. Forrest, *4.2% efficient organic photovoltaic cells with low series resistances*, *Appl. Phys. Lett.* **84**, 3013-3015 (2004).
48. C. M. Ramsdale, J. A. Barker, A. C. Arias, J. D. Mackenzie, R. H. Friend, and N. C., Greenham, *The origin of the open-circuit voltage in polyfluorene-based photovoltaic devices*, *J. Appl. Phys.* **92**, 4266-4270 (2002).
49. V. D. Mihailetchi, P. W. M. Blom, J. C. Hummelen, and M. T. Rispen, *Cathode dependence of the open-circuit voltage of polymer:fullerene bulk heterojunction solar cells*, *J. Appl. Phys.* **94**, 6849-6854 (2003).

50. M. C. Scharber, D. Mühlbacher, M. Koppe, P. Denk, C. Waldauf, A. J. Heeger, and C. J. Brabec, *Design rules for donors in bulk heterojunction solar cells-Towards 10% energy-conversion efficiency*, Adv. Mater. **18**, 789-794 (2006).
51. A. Gadisa, M. Svensson, M. R. Andersson, and O. Inganäs, *Correlation between oxidation potential and open-circuit voltage of composite solar cells based on blends of polythiophenes/fullerene derivative*, Appl. Phys. Lett **84**, 1609-1611 (2004).
52. T. Johansson, W. Mammo, M. Svensson, M. R. Andersson, and O. Inganäs, *Electrochemical bandgaps of substituted polythiophenes*, J. Mater. Chem. **13**, 1316-1323 (2003).
53. H. Sirringhaus, N. Tessler, and R. H. Friend, *Integrated optoelectronic devices based on conjugated polymers*, Science **280**, 1741-1744 (1998).
54. J. Frenkel, *On pre-breakdown phenomena in insulators and electronic semi-conductors*, Phys. Rev. **54**, 647-648 (1938).
55. H. Bässler, *Charge transport in disordered photoconductors a Monte Carlo simulation study*, Phys. Status Solidi (b), **175**, 15-56 (1993).
56. A. Miller, and E. Abrahams, *Impurity conduction at low concentrations*, Phys. Rev. **120**, 745-755 (1960).
57. P. M. Borsenberger, and J. J. Fitzgerald, *Effects of the dipole moment on charge transport in disordered molecular solids*, J. Phys. Chem. **97**, 4815-4819 (1993).
58. Y. Shirota, *Organic materials for electronic and optoelectronic devices*, J. Mater. Chem. **10**, 1-25 (2000).
59. C. Im, H. Bässler, H. Rost, and H. H. Hörhold, *Hole transport in polyphenylenevinylene-ether under bulk photoexcitation and sensitized injection*, J. Chem. Phys. **113**, 3802-3807 (2000).
60. H. C. F. Martens, P. W. M. Blom, and H. F. M. Schoo, *Comparative study of hole transport in poly(p-phenylene vinylene) derivatives*, Phys. Rev. B **61**, 7489-7493 (2000).
61. A. J. Mozer, P. Denk, M. C. Scharber, H. Neugebauer, N. S. Sariciftci, P. Wagner, L. Lutsen, and D. Vanderzande, *Novel regiospecific MDMO-PPV copolymer with improved charge transport for bulk heterojunction solar cells*, J. Phys. Chem. B **108**, 5235-5242 (2004).
62. A. J. Mozer, N. S. Sariciftci, A. Pivrikas, R. Österbacka, G. Juška, L. Brassat, and H. Bässler, *Charge carrier mobility in regioregular poly(3-hexylthiophene) probed by transient conductivity techniques: A comparative study*, Phys. Rev. B **71**, 035214(1)-035214(9) (2005).
63. D.M. Pai, *Transient Photoconductivity in Poly(N-vinylcarbazole)*, J. Chem. Phys. **52**, 2285-2291 (1970).
64. L.B. Schein, A. Peled, and D. Glatz, *The electric field dependence of the mobility in molecularly doped polymers*, J. Appl. Phys. **66**, 686-692 (1989).
65. H. C. F. Martens, H. B. Brom, and P.W.M. Blom, *Frequency-dependent electrical response of holes in poly(p-phenylene vinylene)*, Phys. Rev. B **60**, R8489-R8492 (1999).
66. Y. N. Gartstein, and E. M. Conwell, *High-field hopping mobility in molecular systems with spatially correlated energetic disorder*, Chem. Phys. Lett **245**, 351-358 (1995).
67. S. V. Novikov, D. H. Dunlap, V. M. Kenkre, P. E. Parris, and A. V. Vannikov, *Essential role of correlations in governing charge transport in disordered organic materials*, Phys. Rev. Lett **81**, 4472-4475 (1998).
68. S. V. Rakhmanova, and E. M. Conwell, *Mobility variation with field in conducting polymer films*, Synth. Met. **116**, 389-391 (2001).

69. V. D. Mihailetschi, J. K. J. van Duren, P. W. M. Blom, J. C. Hummelen, René A. J. Janssen, J. M. Kroon, M. T. Rispens, W. Jan H. Verhees, and M. M. Wienk, *Electron transport in a methanofullerene*, Adv. Func. Mater. **13**, 43-46 (2003).
70. P. E. Parris, V. M. Kenkre, and D. H. Dunlap, *Nature of charge carriers in disordered molecular solids: Are polarons compatible with observations*, Phys. Rev. Lett. **87**, 126601(1)-126601(4) (2001).
71. T. Kreouzis, D. Poplavskyy, S. M. Tuladhar, M. C.-Quiles, J. Nelson, A. J. Campbell, and D. D. C. Bradley, *Temperature and field dependence of hole mobility in poly(9,9-dioctylfluorene)*, Phys. Rev. B **73**, 235201(1)-235201(15) (2006).
72. A. B. Walker, A. Kambili, and S. J. Martin, *Electrical transport modelling in organic electroluminescent devices*, J. Phys. Condens. Matter **14**, 9825-9876 (2002).
73. W. E. Spear, *Drift mobility techniques for the study of electrical transport properties in insulating solids*, J. Non-Cryst. Solids **1**, 197-214 (1969).
74. D. Hertel, H. Bässler, U. Scherf, and H. H. Hörhold, *Charge carrier transport in conjugated polymers*, J. Chem. Phys. **110**, 9214-9222 (1999).
75. G. Juška, K. Arlauskas, M. Viliunas, and J. Kočka, *Extraction current transients: New method of study of charge transport in microcrystalline silicon*, Phys. Rev. Lett. **84**, 4946-4949 (2000).
76. G. Juška, K. Arlauskas, M. Viliunas, K. Genevicius, R. Österbacka, and H. Stubb, *Charge transport in p-conjugated polymers from extraction current transients*, Phys. Rev. B **62**, R16235-R16238 (2000).
77. R. Österbacka, A. Pivrikas, G. Juška, K. Genevicius, K. Arlauskas, and H. Stubb, *Mobility and density relaxation of photogenerated charge carriers in organic materials*, Curr. Appl. Phys. **4**, 534-538 (2004).
78. K. Pichler, C. P. Jarrett, R. H. Friend, B. Ratier, and A. Moliton, *Field-effect transistors based on poly(p-phenylene vinylene) doped by ion implantation*, J. Appl. Phys. **77**, 3523-3527 (1995).
79. G. Wang, J. Swensen, D. Moses, and A. J. Heeger, *Increased mobility from regioregular poly(3-hexylthiophene) field-effect transistors*, J. Appl. Phys. **93**, 6137-6141 (2003).
80. C. Tanase, E. J. Meijer, P. W. M. Blom, and D. M. de Leeuw, *Unification of the hole transport in polymeric field-effect transistors and light-emitting diodes*, Phys. Rev. Lett. **91**, 216601(1)-216601(4) (2003).
81. C. Tanase, P. W. M. Blom, and D. M. de Leeuw, *Origin of the enhanced space-charge-limited current in poly(p-phenylene vinylene)*, Phys. Rev. B **70**, 193202(1)-193202(4) (2004).
82. M. A. Lampert, and P. Mark, *Current Injection in Solids*, Academic, New York, (1970).
83. P. W. M. Blom, M. J. M. de Jong, and J. J. M. Vlegaar, *Electron and hole transport in poly(p-phenylene vinylene) devices*, Appl. Phys. Lett. **68**, 3308, 3310 (1996).
84. I. D. Parker, *Carrier tunneling and device characteristics in polymer light-emitting diodes*, J. Appl. Phys. **75**, 1656-1666 (1994).
85. S. M. Sze, *Physics of Semiconductor Devices*, New York:Wiley (1981).
86. M. A. Baldo, and S. R. Forrest, *Interface-limited injection in amorphous organic semiconductors*, Phys. Rev. B **64**, 085201(1)-085201(17) (2001).
87. U. Wolf, V. I. Arkhipov, and H. Bässler, *Current injection from a metal to a disordered hopping system. I. Monte Carlo simulation*, Phys. Rev. B **59**, 7507-7513 (1999).
88. Yu. N. Gartstein, and E. M. Conwell, *Field-dependent thermal injection into a disordered molecular insulator*, Chem. Phys. Lett. **255**, 93-98 (1996).

89. S. V. Novikov, and G. G. Malliaras, *Roughness-induced energetic disorder at the metal/organic interface*, Phys. Rev. B **73**, 033302(1)- 033302(4) (2006).
90. A. J. Campbell, D. D. C. Bradley, and D. G. Lidzey, *Space-charge limited conduction with traps in poly(phenylene vinylene) light emitting diodes*, J. Appl. Phys. **82**, 6326-6342 (1997).
91. E. Perzon, X. Wang, F. Zhang, W. Mammo, J. L. Delgado, P. de la Cruz, O. Inganäs, F. Langa, and Mats .R. Andersson, *Design, synthesis and properties of low band gap polyfluorenes for photovoltaic devices*, Synth. Met. **154**, 53-56 (2005).
92. O. Inganäs, M. Svensson, F. Zhang, A. Gadisa, N. K. Persson, X. Wang, and Mats. R. Andersson, *Low bandgap alternating polyfluorene copolymers in plastic photodiodes and solar cells*, Appl. Phys. A-Mater.Sci. Process. **79**, 31-35 (2004).
93. X. Wang, E. Perzon, J. L. Delgado, P. de la Cruz, F. Zhang, F. Langa, M. R. Andersson, and O. Inganäs, *Infrared photocurrent spectral response from plastic solar cell with low-band-gap polyfluorene and fullerene derivative*, Appl. Phys. Lett. **85**, 5081-5083 (2004).
94. X. Wang, E. Perzon, W. Mammo, F. Oswald, S. Admassie, N-K. Persson, F. Langa, M. R. Andersson, and O. Inganäs, *Polymer solar cells with low-bandgap polymers blended with C₇₀-derivative give photocurrent at 1 μm*, Thin Solid Films **511-512**, 576-580 (2006).
95. K. Yoshino, Y. Manda, K. Sawada, M. Onoda, R. Sugomoto, *Anomalous dependences of luminescence of poly(3-alkylthiophene) on temperature and alkyl chain length*, Solid State Commun. **69**, 143-146 (1989).
96. A. C. Grimsdale, P. LecÈre, R. Lazzaroni, J. D. Mackenzie, C. Murphy, S. Setayesh, C. Silva, R. H. Friend, and K. Müllen, *Correlation Between Molecular Structure, Microscopic Morphology, and Optical Properties of Poly(tetraalkylindenofluorene)s*, Adv. Funct. Mater. **12**, 729-733 (2002).
97. C. Tanase, J. Wildeman, P. W. M. Blom, M. E. M. Benito, D. M. de Leeuw, A. J. J. M. van Breemen, P. T. Herwig, C. H. T. Chlon, J. Sweelssen, and H. F. M. Schoo, *Optimization of the charge transport in poly(phenylene vinylene) derivatives by processing and chemical modification*, J. Appl. Phys. **97**, 123703(1)-123703(6) (2005).
98. A. Gadisa, F. Zhang, D. Sharma, M. Svensson, Mats R. Andersson, and O. Inganäs, *Improvements of fill factor in solar cells based on blends of polyfluorene copolymers as electron donors*, Thin Solid Films, In press.
99. J. K. J. van Duren, X. Yang, J. Loose, C. W. T. Bulle-Lieuwma, A. B. Sieval, J. C. Hummelen, and René A. J. Janssen, *Relating the morphology of poly(p-phenylene vinylene)/methanofullerene blends to solar-cell performance*, Adv. Funct. Mater. **14**, 425-434 (2004).
100. H. Hoppe, M. Niggemann, C. Winder, J. Kraut, R. Hiesgen, A. Hinsch, D. Meissner, and N. S. Sariciftci, *Nanoscale morphology of conjugated polymer/fullerene-based bulk-heterojunction solar cells*, Adv. Funct. Mater. **14**, 1005-1011 (2004).
101. S. M. Tuladhar, D. Poplavskyy, S. A. Choulis, J. R. Durrant, D. D. C. Bradley, and J. Nelson, *Ambipolar Charge Transport in Films of Methanofullerene and Poly(phenylenevinylene)/Methanofullerene Blends*, J. Nelson, Adv. Funct. Mater. **15**, 1171-1182 (2005).
102. S. A. Choulis, J. Nelson, Y. Kim, D. Poplavskyy, T. Kreouzis, J. R. Durrant, and D. D. C. Bradley, *Investigation of transport properties in polymer/fullerene blends using time-of-flight photocurrent measurements*, Appl. Phys. Lett. **83**, 3812-3814 (2003).

103. C. Melzer, E. J. Koop, V. D. Mihailetchi, and P. W. M. Blom, *Hole transport in poly(phenylene vinylene)/methanofullerene bulk-heterojunction solar cells*, Adv. Func. Mater. **14**, 865-870 (2004).
104. V. D. Mihailetchi, L. J. A. Koster, P. W. M. Blom, C. Melzer, B. de Boer, J. K. J. van Duren, and René A. J. Janssen, *Compositional dependence of the performance of poly(p-phenylene vinylene):methanofullerene bulk-heterojunction solar cells*, Adv. Func. Mater. **15**, 795-801 (2005).
105. L. M. Andersson, and O. Inganäs, *Acceptor influence on hole mobility in fullerene blends with alternating copolymers of fluorene*, Appl. Phys. Lett. **88**, 082103(1)-082103(3) (2006).
106. M. R.-Reyes, K. Kim, and D. L. Carroll, *High-efficiency photovoltaic devices based on annealed poly(3-hexylthiophene) and 1-(3-methoxycarbonyl)-propyl-1-phenyl-(6,6)C₆₁ blends*, Appl. Phys. Lett. **87**, 083506(1)-083506(3) (2005).
107. V. D. Mihailetchi, H. Xie, B. de Boer, L. Jan A. Koster, and P. W. M. Blom, *Charge transport and photocurrent generation in poly(3-hexylthiophene):methanofullerene bulk-heterojunction solar cells*, Adv. Funct. Mater. **16**, 699-708 (2006).
108. A. Gadisa, X. Wang, S. Admassie, E. Perzon, F. Oswald, F. Langa, Mats R. Andersson, and O. Inganäs, *Stoichiometry dependence of charge transport in polymer/methanofullerene and polymer/C₇₀ derivative based solar cells*, Org. Electron. **7**, 195-204 (2006).
109. K. G. Jespersen, F. Zhang, A. Gadisa, V. Sundström, A. Yartsev, and O. Inganäs, *Charge formation and transport in bulk-heterojunction solar cells based on alternating polyfluorene copolymers blended with fullerenes*, Org. Electron. **7**, 235-242 (2006).
110. T. D. Anthopoulos, C. Tanase, S. Setayesh, E. J. Meijer, J. C. Hummelen, P. W. M. Blom, and D. M. De Leeuw, *Ambipolar organic field-effect transistors based on a solution processed methanofullerene*, Adv. Mater. **16**, 2174-2179 (2004).
111. A. Gadisa, X. Wang, K. Tvingstedt, F. Oswald, F. Langa, and O. Inganäs, *Bipolar transport and infrared light emission in C₆₀ and C₇₀ derivative electron acceptors*, Appl. Phys. Lett., submitted.
112. M. A. Baldo, and S. R. Forrest, *Interface-limited injection in amorphous organic semiconductors*, Phys. Rev. B **64**, 085201(1)-085201(17) (2001).
113. L. Lindell, M. P. de Jong, W. Osikowicz, R. Lazzaroni, M. Berggren, W. R. Salaneck, and, X. Crispin, *Characterization of the interface dipole at the paraphenylenediamine-nickel interface: A joint theoretical and experimental study*, J. Chem. Phys. **122**, 084712(1)-084712-(12) (2005).
114. C. M Björström, A. Bernasik, J. Rysz, A. Budkowski, S. Nilsson, M. Svensson, Mats R Andersson, K. O. Magnusson, and E. Moons, *Multilayer formation in spin-coated thin films of low-bandgap polyfluorene:PCBM blends*, J. Phys.: Condens. Matter **17**, L529-L534 (2005).
115. S. A. Carter, M. Angelopoulos, S. Karg, P. J. Brock, and J. C. Scott, *Polymeric anodes for improved polymer light-emitting diode performance*, Appl. Phys. Lett. **70**, 2067-2069 (1997).
116. S. K. M. Jönsson, J. Birgeron, X. Crispin, G. Greczynski, W. Osikowicz, A. W. Denier van der Gon, W. R. Salaneck, and M. Fahlman, *The effects of solvents on the morphology and sheet resistance in poly(3,4-ethylenedioxythiophene)-polystyrenesulfonic acid (PEDOT-PSS) films*, Synth. Met. **139**, 1-10 (2003).
117. S. Ghosh, and O. Inganäs, *Networks of electron-conducting polymer in matrices of ion-conducting polymers: Applications to fast electrodes*, Electrochem. Solid State Lett. **3**, 213-215 (2000).

118. B. D. Martin, N. Nikolov, S. K. Pollack, A. Sapirgin, R. Shashidhar, F. Zhang, and P.A. Heiney, *Hydroxylated secondary dopants for surface resistance enhancement in transparent poly(3,4-ethylenedioxythiophene)-poly(styrenesulfonate) thin films*, Synth. Met. **142**, 187–193 (2004).
119. J. Y. Kim, J. H. Jung, D. E. Lee, and J. Joo, *Enhancement of electrical conductivity of poly(3,4-ethylenedioxythiophene)/poly(4-styrenesulfonate) by a change of solvents*, Synth. Met **126**, 311–316 (2002).
120. F. Zhang, A. Gadisa, O. Inganäs, M. Svensson, and Mats. R. Andersson, *Influence of buffer layers on the performance of polymer solar cells*, Appl. Phys. Lett. **84**, 3906-3908 (2004).
121. B. W.-Jensen, and K. West, *Vapor-phase polymerization of 3,4-ethylenedioxythiophene: A route to highly conducting polymer surface layers*, Macromolecules **37**, 4538-4543 (2004).
122. S. Admassie, F. Zhang, A. G. Manoj, M. Svensson, M. R. Andersson, and O. Inganäs, *A polymer photodiode using vapour-phase polymerized PEDOT as an anode*, Sol. Energy Mater. Sol. Cells **90**, 133–141 (2006).
123. B. W.-Jensen, and F. C. Krebs, *High-conductivity large-area semi-transparent electrodes for polymer photovoltaics by silk screen printing and vapour-phase deposition*, Sol. Energy Mater. Sol. Cells **90**, 123-132 (2006).
124. A. Gadisa, K. Tvingstedt, S. Admassie, L. Lindell, X. Crispin, Mats R. Andersson, W.R Salaneck, Olle Inganäs, *Transparent polymer cathode for organic photovoltaic devices*, Synth. Met. **156**, 1102–1107 (2006).
125. M. Glatthaar, M. Niggemann, B. Zimmermann, P. Lewer, M. Riede, A. Hinsch and J. Luther, *Organic solar cells using inverted layer sequence*, Thin Solid Films, **491**, 298-300 (2005).
126. J. Zaumseil, T. Someya, Z. Bao, Y.-L. Loo, R. Cirelli, and J. A. Rogers, *Nanoscale organic transistors that use source/drain electrodes supported by high resolution rubber stamps*, App. Phys. Lett. **82**, 793-795 (2003).
127. T.-W. Lee, J. Zaumseil, Z. Bao, J. W. P. Hsu, and J. A. Rogers, *Organic light-emitting diodes formed by soft contact lamination*, Proc. Natl. Acad. Sci. U. S. A. **101**, 429-433 (2004).
128. D. A. Bernards, T. Biegala, Z. A. Samuels, J. D. Slinker, G. G. Malliaras, S. F. Torres, H. D. Abruña, and J. A. Rogers, *Organic light-emitting devices with laminated top contacts*, App. Phys. Lett. **84**, 3675-3677 (2004).
129. T.-W. Lee, J. Zaumseil, S. H. Kim, and J. W. P. Hsu, *High-efficiency soft-contact-laminated polymer light-emitting devices with patterned electrodes*, Adv. Mater. **16**, 2040-2045 (2004).
130. J.-Hyun Kim, M. Yoneya, J. Yamamoto, and H. Yokoyama, *Nano-rubbing of a liquid crystal alignment layer by an atomic force microscope: a detailed characterization*, Nanotechnology **13**, 133–137 (2002).
131. H. Sato, H. Fujikake, H. Kikuchi, Y. Iino, M. Kawakita, and Y. Tsuchiya, *Fluorinated polymer alignment layers formed at low temperature for plastic-substrate-based liquid crystal devices*, Jpn. J. Appl. Phys. **40**, L53-L55 (2001).
132. M. Grell, and D. D. C. Bradley, *Polarized luminescence from oriented molecular materials*, Adv. Mater. **11**, 895-905 (1999).
133. V. K. Gupta, and N. L. Abbott, *Design of surfaces for patterned alignment of liquid crystals on planar and curved substrates*, Science **276**, 1533-1536 (1997).
134. B. Scharfel, V. Wachtendorf, M. Grell, D. D. C. Bradley, and M. Hennecke, *Polarized fluorescence and orientational order parameters of a liquid-crystalline conjugated polymer*, Phys. Rev. B **60**, 277-283 (1999).

135. T. Miteva, A. Meisel, W. Knoll, H. G. Nothofer, U. Scherf, D. C. Müller, K. Meerholz, A. Yasuda, and D. Neher, *Improving the performance of polyfluorene-based organic light-emitting diodes via end-capping*, *Adv. Mater.* **13**, 565-570 (2001).
136. M. Jandke, P. Strohriegel, J. Gmeiner, W. Brütting, and M. Schwoerer, *Polarized electroluminescence from rubbing-aligned poly(p-phenylenevinylene)*, *Adv. Mater.* **11**, 1518-1521 (1999).
137. S.-Wen Chang, A.-Kuo Li, C.-Wei Liao, and C.-Shu Hsu, *Polarized blue emission based on a side chain liquid crystalline polyacrylate containing bis-tolane side groups*, *Jpn. J. Appl. Phys.* **41**, 1374-1378 (2002).
138. S. W. Culligan, Y. Geng, S. H. Chen, K. Klubek, K. M. Vaeth, and C.W. Tang, *Strongly polarized and efficient blue organic light-emitting diodes using monodisperse glassy nematic oligo(fluorene)s*, *Adv. Mater.* **15**, 1176-1180 (2003).
139. A. Gadisa, and O. Inganäs, *Red and near infrared polarized light emission from polyfluorene copolymers based light emitting diodes*, Manuscript.
140. J. A. Misewich, R. Martel, P. Avouris, J. C. Tsang, S. Heinze, and J. Tersoff, *Electrically induced optical emission from a carbon nanotube FET*, *Science* **300**, 783-786 (2003).